

Distributed Precoding for Satellite-Terrestrial Integrated Networks Without Sharing CSIT: A Rate-Splitting Approach

Doseon Kim, Wonjae Shin, Jeonghun Park, and Dong Ku Kim

arXiv:2309.06325v1 [cs.IT] 12 Sep 2023

Abstract—Satellite-terrestrial integrated networks (STINs) are promising architecture for providing global coverage. In STINs, full frequency reuse between a satellite and a terrestrial base station (BS) is encouraged for enhancing spectral efficiency, which accounts for non-negligible amount of interference. To address the interference management problem in STINs, this paper proposes a novel distributed precoding method. Key features of our method are: i) a rate-splitting (RS) strategy is incorporated for efficient interference management, ii) precoders are designed in a distributed way without sharing channel state information between a satellite and a terrestrial BS. Specifically, to design precoders in a distributed fashion, we put forth a spectral efficiency decoupling technique. This technique disentangles the total spectral efficiency into two distinct terms, each dependent solely on the satellite’s precoder and the terrestrial BS’s precoder, respectively. Then, to resolve the non-smoothness raised by adopting the RS strategy, we approximate the spectral efficiency expression as a smooth function; thereafter we develop a generalized power iteration inspired optimization algorithm built based on the first-order optimality condition. Simulation results demonstrate that the proposed method improves the spectral efficiency (around 20 ~ 29%) compared to existing distributed precoding schemes.

Index Terms—Satellite-terrestrial integrated networks, rate-splitting, distributed precoding, generalized power iteration

I. INTRODUCTION

Managing inter-cell interference (ICI) is one of long-standing problems in cellular networks. Due to an inherent characteristic of resource reuse, ICI fundamentally limits the rate performance [1]; thus, efficiently handling the interference is a key to achieve the high spectral efficiency of cellular networks. So far, numerous studies have been conducted to mitigate ICI by using multi-cell multiple-input multiple-output (MIMO) cooperative transmission [2]. In most of MIMO cooperation techniques, a key principle is designing precoders in a coordinated fashion (i.e., coordinated precoding), where multiple base stations (BSs) share channel state information at transmitters (CSIT), then obtain their precoders by jointly exploiting shared CSIT.

Recently, with the growing interest in satellite communications, satellite-terrestrial integrated networks (STINs) gain significant attention. One promising scenario of operating

Doseon Kim, Jeonghun Park, and Dong Ku Kim are with the School of Electrical and Electronic Engineering, Yonsei University, Seoul 03722, South Korea (e-mail: kds1018@yonsei.ac.kr; jhpark@yonsei.ac.kr; dkkim@yonsei.ac.kr). Wonjae Shin is with the School of Electrical Engineering, Korea University, Seoul 02841, South Korea (email: wjshin@korea.ac.kr)

STINs is using satellites to serve alienated users left outside of a terrestrial coverage region [3]. In such a scenario, assuming full frequency reuse (FFR) for aggressive spectrum reuse [4], the interference stemming from a satellite is mainly considered as a significant factor to deteriorate the spectral efficiency of STINs [5]. To handle this interference, one may be tempted to apply the widely used coordinated precoding approaches from previous researches that require sharing CSIT between a satellite and a terrestrial BS. Nonetheless, CSIT sharing between a satellite and a terrestrial BS is difficult. Unlike terrestrial BSs connected via wireline transport network of X2, satellites require extra wireless resources for connecting to a terrestrial gateway [5]. For this reason, sharing CSIT in STINs causes significant overheads, which hinders to use the coordinated precoding methods. Accordingly, a desirable way to address the interference in STINs is using a distributed precoding method, where each of satellite and terrestrial BS determines their precoders individually while not sharing CSIT. Motivated by this, we propose a novel distributed precoding method for efficiently managing the interference in STINs.

A. Related Work

In design of distributed downlink precoding, it is infeasible to compute the exact signal-to-interference-plus-noise ratio (SINR) because CSIT sharing is not allowed. To address this, in [6], the signal-to-leakage-plus-noise ratio (SLNR) was considered, which is computed by the ratio between the signal power and the sum of the leakage interference plus the noise power. Here, the leakage interference power indicates the amount of transmit power that a BS incurs to neighboring cells. By doing this, one can readily come up with downlink precoding vectors by taking advantage of equivalence between the SLNR and the uplink SINR, wherein the optimal combiner is well-known as a minimum mean-squared error (MMSE) combiner. In [7]–[9], virtual SINR (VSINR) was proposed and studied, which is an extension of SLNR to multi-point joint transmission setups. Especially, in [9], the Pareto optimal boundary of linear precoding was characterized using VSINR.

Besides the Pareto optimality analysis, practical distributed precoding schemes were also actively investigated. In [10], assuming heterogeneous network scenarios, a per-cell energy efficiency maximization precoding was developed based on weighted MMSE, while restricting the maximum amount of leakage to other cells. SLNR was also introduced to develop precoding methods for maximizing spectral efficiency and

energy efficiency [11]. In [12], the inter-user interference (IUI) term and the other-cell interference term are separated from the sum spectral efficiency by assuming high signal-to-noise ratio (SNR) approximation, by which the distributed precoding scheme was developed for jointly mitigating the IUI and the leakage. In [13], a new metric called signal-to-interference-plus-leakage-plus-noise ratio (SILNR) was proposed, which primarily differs from SLNR in how it handles the IUI while considering the product term of leakage interference. [13] showed that for a large number of antennas at a BS, SILNR-based distributed precoding provides an equivalent sum spectral efficiency to the coordinated precoding scheme. In [14], a distributed precoding method with network virtualization was proposed in a semi-closed form.

Despite the abundant prior work of distributed precoding methods, the existing schemes are inherently limited in an information-theoretical sense. To be specific, the existing methods implicitly assume a treating interference as noise (TIN) based decoding strategy, wherein each user only decodes its own signal without using an advanced treatment to interference. From an information theoretical perspective, TIN is optimal in a weak interference regime [15], which achieves quasi-optimal spectral efficiency [16]. However, in STINs, it is infeasible for a terrestrial receiver to perfectly estimate the satellite interference channels due to the large propagation distance and severe randomness, such as large Doppler effects. As a result, it cannot sufficiently suppress interference from the satellite and may remain in a strong interference region. In such a strong interference regime, a terrestrial receiver using TIN loses its optimality and needs a proactive decoding strategy, such as rate-splitting (RS) [17].

From such a motivation, there exist some prior work that employed RS in STINs based on satellite-terrestrial BS coordination. For instance, in [5], two approaches were proposed: one is a coordinated approach that shares CSIT, the other is a cooperative approach that shares not only CSIT but also transmitted data. For both approaches, a precoding scheme incorporating RS was proposed to mitigate the interference in STINs. In [18], a multi-layer interference management scheme was proposed in the multiple satellite network, where the RS strategy is implemented across different satellites through CSIT sharing. To use such methods [5], [18], however, CSIT or transmitted data should be shared between a satellite and a terrestrial BS. As mentioned above, this sharing is not easy in STINs due to the lack of a dedicated link between a satellite and a terrestrial BS. As a result, a precoding method that i) incorporates RS and ii) requires no CSIT sharing is needed to develop. This serves as a primary motivation of our work.

B. Contributions

In this paper, we consider the downlink system of STINs. In our scenario, a terrestrial BS serves terrestrial users (TUs) located within its coverage, while a low-earth-orbit (LEO) satellite serves satellite users (SUs) situated beyond the coverage range of the terrestrial BS. For this reason, the terrestrial BS does not impose any interference to the SUs. On the contrary, the satellite can incur the interference to certain

TUs in some regions reachable by the LEO satellite signal. Given this setup, we propose a distributed precoding method to efficiently handle the interference without sharing CSIT. Key features of our method are summarized as follows.

- **RS strategy:** Our precoding method incorporates the RS strategy. The RS strategy enables the SUs and a part of the TUs to mitigate the interference coming from the satellite by using successive interference cancellation (SIC). To this end, the messages intended to the SUs are split into a common and a private parts, wherein the common parts are jointly encoded into a common stream. The common stream is constructed to be decoded by the SUs and some of the TUs affected by the LEO satellite signal. To be specific, the SUs and a part of the TUs first decode the common stream while treating other streams as noise, and eliminate the common stream with SIC, thereafter decode the private stream. Upon this decoding process of the RS strategy, we derive a lower bound on the spectral efficiencies by considering the effects on the imperfect CSIT and the RS decoding condition. Subsequently, we formulate the sum spectral efficiency maximization problem.
- **Spectral efficiency decoupling:** Addressing the posed problem necessitates a coordinated approach involving CSIT sharing between the LEO satellite and the terrestrial BS. To solve this problem in a distributed fashion, we introduce a novel spectral efficiency decoupling technique. Specifically, we take average on IUI terms over the randomness related to incomplete knowledge of the channel fading process. This allows us to decouple the spectral efficiencies into two separated terms, each of which is only associated with a terrestrial BS precoding vector and satellite precoding vector, respectively. Based on this decoupling, we transform the original problem into the distributed precoding optimization problem.
- **Distributed precoding optimization:** Even after transforming the original problem into the distributed problem, finding its solution is challenging since the problem is non-convex and non-smooth. To address this, we first approximate the objective function by using the LogSum-Exp (LSE) technique. Then we characterize the first-order Karush–Kuhn–Tucker (KKT) conditions and cast these as generalized nonlinear eigenvalue problems. We show that finding the principal eigenvector of these nonlinear eigenvalue problems is equivalent to finding the local optimal solution. Leveraging this, we propose an iterative algorithm named STIN-generalized power iteration (STIN-GPI).
- **Simulations:** Through link-level and system-level simulations, we numerically demonstrate that the proposed STIN-GPI algorithm outperforms the current state-of-the-art distributed precoding methods.

II. SYSTEM MODELS

A. Network Model

We consider a STIN that consists of a LEO satellite and a terrestrial BS. We focus on the downlink system with FFR,

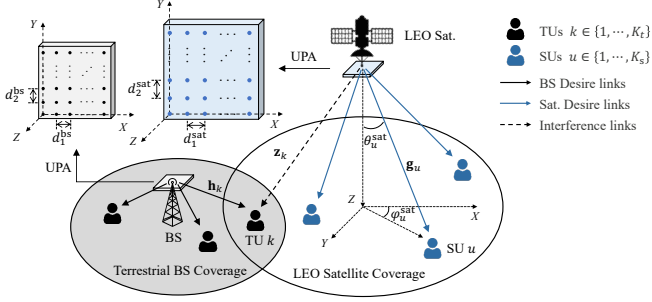


Fig. 1. The system model of the STIN and the geometrical model of UPA.

wherein both the LEO satellite and the terrestrial BS use the same frequency band. As illustrated in Fig. 1, there exist K_s SUs and K_t TUs, and the total number of users is $K = K_s + K_t$. We denote $\mathcal{K}_s = \{1, \dots, K_s\}$ as a set of the SUs with $|\mathcal{K}_s| = K_s$ and $\mathcal{K}_t = \{1, \dots, K_t\}$ as a set of the TUs with $|\mathcal{K}_t| = K_t$. We assume that the TUs are associated with the terrestrial BS and the SUs are connected to the LEO satellite. In our setup, the terrestrial BS does not incur any interference to the SUs since all the SUs are located outside of the coverage region of the terrestrial BS. On the contrary, the LEO satellite can incur interference to some TUs¹ when they are located within the coverage region of the LEO satellite [5] as shown in Fig. 1. We define a subset of the TUs that experiences the interference from the LEO satellite as $\mathcal{K}_t^{\text{int}} \subseteq \mathcal{K}_t$, where $|\mathcal{K}_t^{\text{int}}| = K_t^{\text{int}}$. The total number of users in the LEO satellite coverage is $K^{\text{sat}} = K_t^{\text{int}} + K_s$. If $K_t = K_s = 1$ and $\mathcal{K}_t^{\text{int}} = \mathcal{K}_t$, the considered setup corresponds to the Z channel [19]. Our interference environment is an extension of the Z channel for $K_t \geq 1$, $K_s \geq 1$, and $\mathcal{K}_t^{\text{int}} \subseteq \mathcal{K}_t$.

The LEO satellite is equipped with the uniform planar arrays (UPAs) with M_1 and M_2 array elements in the x -axis and y -axis, respectively. The total number of antennas at the LEO satellite is $M \triangleq M_1 M_2$. The terrestrial BS is also equipped with $N \triangleq N_1 N_2$ number of UPAs, where it consists of N_1 and N_2 array elements in the x -axis and y -axis, respectively. Furthermore, we assume that all users are equipped with a single antenna.

B. Channel Model

1) *Satellite Channel*: For modeling satellite channel, we use a widely-adopted multi-path channel model. Using a ray-tracing based modeling, the complex baseband channel impulse response of the downlink satellite channel vector for SU u , $\forall u \in \mathcal{K}_s$, denoted by $\mathbf{g}_u(t, \tau) \in \mathbb{C}^M$, is written as

$$\mathbf{g}_u(t, \tau) = \frac{1}{\sqrt{L_s}} \sum_{\ell=0}^{L_s-1} g_u e^{j2\pi\nu_{u,\ell}t} \delta(\tau - \tau_{u,\ell}) \mathbf{a}(\theta_{u,\ell}^{\text{sat}}, \varphi_{u,\ell}^{\text{sat}}, \mathcal{D}^{\text{sat}}), \quad (1)$$

where L_s is the number of propagation paths, g_u is the complex channel gain, $\nu_{u,\ell}$ is the Doppler shift, $\tau_{u,\ell}$ is the propagation delay, and $\mathbf{a}(\cdot, \cdot, \cdot)$ is the array response vector

¹If SUs enter the terrestrial coverage region, they change their association to the terrestrial BS and become TUs [5].

corresponding to the ℓ -th path of SU u 's channel. Note that $\theta_{u,\ell}^{\text{sat}}$ and $\varphi_{u,\ell}^{\text{sat}}$ represent the vertical and horizontal angle-of-departure (AoD), respectively and $\mathcal{D}^{\text{sat}} = \{d_1^{\text{sat}}, d_2^{\text{sat}}\}$ is a set of the satellite's UPA inter-element spacing in the x -axis and y -axis, respectively. Without loss of generality, we assume that $\ell = 0$ indicates the first arriving path and $\ell = L_s - 1$ indicates the last arriving path at the satellite, resulting in $\tau_{u,0} \leq \tau_{u,1} \leq \dots \leq \tau_{u,L_s-1}$.

Doppler shift: We first explain the Doppler shift $\nu_{u,\ell}$. Typically, the Doppler shift for the LEO satellite channel is much larger compared to the terrestrial channel because of the high mobility of the LEO satellite. Fortunately, we can exploit a favorable characteristic of the Doppler shift in the LEO satellite channel; each path has almost identical Doppler, i.e., $\nu_{u,\ell} = \nu_u$. This is because the traveling distances of each path can be assumed to be approximately the same due to the high altitude of the LEO satellite.² This allows to compensate the Doppler shift at the LEO satellite by multiplying $e^{-j2\pi\nu_u t}$ to the received signal as presented in [20]–[23].

Delay: The propagation delay is also an important issue in LEO satellite communications because of a long propagation distance. Thanks to the line-of-sight (LoS)-like characteristic of LEO satellite channels [20], [21], it is not difficult to compensate the delay effects. Specifically, denoting the delay spread as $\tau^{\text{sp}} = \tau_{u,L_s-1} - \tau_{u,0}$, τ^{sp} is rather smaller than that of terrestrial communications since the traveling distances between each propagation path are very similar, which makes the LEO channel rather LoS-like. This is also confirmed with the measurement results [24], [25]. Therefore, if the receiver can achieve symbol synchronization by shifting time for a minimum delay of $\tau_{u,0}$, the delay spread can be readily resolved by using the typical orthogonal frequency division multiplex (OFDM) technique as reported in [20]–[23].

Array response vector: Incorporating the LoS-like characteristic of a LEO satellite channel, we have $\mathbf{a}(\theta_{u,\ell}^{\text{sat}}, \varphi_{u,\ell}^{\text{sat}}, \mathcal{D}^{\text{sat}}) \simeq \mathbf{a}(\theta_u^{\text{sat}}, \varphi_u^{\text{sat}}, \mathcal{D}^{\text{sat}})$ for all $0 \leq \ell \leq L_s - 1$. As a result, the effective LEO satellite channel that SU u experiences in one OFDM symbol block is given by

$$\mathbf{g}_u = \tilde{g}_u \mathbf{a}(\theta_u^{\text{sat}}, \varphi_u^{\text{sat}}, \mathcal{D}^{\text{sat}}), \quad (2)$$

where \tilde{g}_u is the effective channel gain after Doppler and delay compensation. Since the LEO satellite channel is nearly LoS, not much spatial randomness exists in \tilde{g}_u . To reflect this, we model \tilde{g}_u by Rician fading. To be specific, $\tilde{g}_u \sim \mathcal{CN}\left(\sqrt{\frac{\kappa_s \alpha_u}{1+\kappa_s}}, \frac{\alpha_u}{1+\kappa_s}\right)$, where $\alpha_u = \frac{G_{\text{sat}} G_u}{k_B T_n B_w} \left(\frac{c}{4\pi f_c d_0^{\text{sat}}}\right)^2$ is the channel power of SU u considering free-space path loss. Here, c is the speed of light, f_c is the carrier frequency, d_0^{sat} denotes the altitude of the LEO satellite, k_B is the Boltzmann constant, T_n is the noise temperature and B_w is the system bandwidth, G_{sat} and G_u respectively represent the antenna gains of the transmitter and the receiver, and κ_s determines the ratio between the deterministic and random components. As $\kappa_s \rightarrow \infty$, \tilde{g}_u becomes a constant, while $\kappa_s \rightarrow 0$, \tilde{g}_u is

²In practice, the Doppler shift can be varied over time due to moving direction of the satellite keeps changing. Taking into account this variation of Doppler shift is, however, beyond the scope of our paper. Thus we assume perfect knowledge on the Doppler shift.

distributed as Rayleigh fading. We note that all of our channel modeling assumptions corresponds to [20], [21], [23], [26].

Now we elaborate on the array response vector. In (2), the array response vector $\mathbf{a}(\theta_u^{\text{sat}}, \varphi_u^{\text{sat}}, \mathcal{D}^{\text{sat}}) \in \mathbb{C}^M$ is given by

$$\mathbf{a}(\theta_u^{\text{sat}}, \varphi_u^{\text{sat}}, \mathcal{D}^{\text{sat}}) = \mathbf{a}_h(\theta_u^{\text{sat}}, \varphi_u^{\text{sat}}, d_1^{\text{sat}}) \otimes \mathbf{a}_v(\theta_u^{\text{sat}}, d_2^{\text{sat}}), \quad (3)$$

where \otimes denotes the Kronecker product, the horizontal steering vector $\mathbf{a}_h(\theta_u^{\text{sat}}, \varphi_u^{\text{sat}}, d_1^{\text{sat}}) \in \mathbb{C}^{M_1}$ and the vertical steering vector $\mathbf{a}_v(\theta_u^{\text{sat}}, d_2^{\text{sat}}) \in \mathbb{C}^{M_2}$ are

$$\mathbf{a}_h(\theta_u^{\text{sat}}, \varphi_u^{\text{sat}}, d_1^{\text{sat}}) = \left[e^{-j\frac{2\pi}{\lambda}\left(\frac{M_1-1}{2}\right)d_1^{\text{sat}} \sin \theta_u^{\text{sat}} \cos \varphi_u^{\text{sat}}}, \dots, e^{+j\frac{2\pi}{\lambda}\left(\frac{M_1-1}{2}\right)d_1^{\text{sat}} \sin \theta_u^{\text{sat}} \cos \varphi_u^{\text{sat}}} \right]^T, \quad (4)$$

$$\mathbf{a}_v(\theta_u^{\text{sat}}, d_2^{\text{sat}}) = \left[e^{-j\frac{2\pi}{\lambda}\left(\frac{M_2-1}{2}\right)d_2^{\text{sat}} \cos \theta_u^{\text{sat}}}, \dots, e^{+j\frac{2\pi}{\lambda}\left(\frac{M_2-1}{2}\right)d_2^{\text{sat}} \cos \theta_u^{\text{sat}}} \right]^T. \quad (5)$$

The channel matrix between the LEO satellite and SUs is denoted by $\mathbf{G} = [\mathbf{g}_1, \dots, \mathbf{g}_{K_s}] \in \mathbb{C}^{M \times K_s}$.

Similar to the above, we can also characterize the interfering channel from the LEO satellite to TUs in $\mathcal{K}_t^{\text{int}}$. Applying the equivalent treatments to the Doppler and the delay, the effective interference channel experienced by TU k , $\forall k \in \mathcal{K}_t^{\text{int}}$, denoted by $\mathbf{z}_k \in \mathbb{C}^M$, is presented by

$$\mathbf{z}_k(t, \tau) = \frac{1}{\sqrt{L_s}} \sum_{\ell=0}^{L_s-1} z_{k,\ell} e^{j2\pi\nu_{k,\ell}t} \delta(\tau - \tau_{k,\ell}) \mathbf{a}(\theta_{k,\ell}^{\text{sat}}, \varphi_{k,\ell}^{\text{sat}}, \mathcal{D}^{\text{sat}}) \\ = \tilde{z}_k \mathbf{a}(\theta_k^{\text{sat}}, \varphi_k^{\text{sat}}, \mathcal{D}^{\text{sat}}) = \mathbf{z}_k, \quad (6)$$

where \tilde{z}_k is the effective channel gain, which follows $\tilde{z}_k \sim \mathcal{CN}\left(\sqrt{\frac{\kappa_s \alpha_k}{1+\kappa_s}}, \frac{\alpha_k}{1+\kappa_s}\right)$. The interfering channel matrix between the LEO satellite and TUs in $\mathcal{K}_t^{\text{int}}$ is defined as $\mathbf{Z} = [\mathbf{z}_1, \dots, \mathbf{z}_{K_t^{\text{int}}}] \in \mathbb{C}^{M \times K_t^{\text{int}}}$.

2) *Terrestrial Channel*: In the terrestrial channel, we assume there is no LoS component by considering dense urban scenarios where large-scale blockages such as buildings are densely placed. Assuming that there are L_t scatters contributing the Non-LoS components, the channel vector $\mathbf{h}_k \in \mathbb{C}^N$ between the terrestrial BS and TU k is given by

$$\mathbf{h}_k = \frac{1}{\sqrt{L_t}} \sum_{\ell=1}^{L_t} h_{k,\ell} \mathbf{a}_h(\theta_{k,\ell}^{\text{bs}}, \varphi_{k,\ell}^{\text{bs}}, d_1^{\text{bs}}) \otimes \mathbf{a}_v(\theta_{k,\ell}^{\text{bs}}, d_2^{\text{bs}}), \quad (7)$$

where $h_{k,\ell}$ is the complex channel gain of ℓ -th path, and it follows $\mathcal{CN}(0, \beta_k)$ which considers the channel power $\beta_k = \frac{G_{\text{bs}} G_k}{k_B T_n B_w} \left(\frac{c}{4\pi f_c}\right)^2 \left(\frac{1}{d_k^{\text{bs}}}\right)^\rho$. Here, d_k^{bs} is the distance between the terrestrial BS and TU k , and ρ is the path loss exponent. We denote that $\theta_{k,\ell}^{\text{bs}}$ and $\varphi_{k,\ell}^{\text{bs}}$ as the vertical AoD and the horizontal AoD for the ℓ -th path and $\mathcal{D}^{\text{bs}} = \{d_1^{\text{bs}}, d_2^{\text{bs}}\}$ as a set of the terrestrial BS's UPA inter-element spacing in the x -axis and y -axis, respectively. Here, the horizontal steering

vector $\mathbf{a}_h(\theta_{k,\ell}^{\text{bs}}, \varphi_{k,\ell}^{\text{bs}}, d_1^{\text{bs}}) \in \mathbb{C}^{N_1}$ and the vertical steering vector $\mathbf{a}_v(\theta_{k,\ell}^{\text{bs}}, d_2^{\text{bs}}) \in \mathbb{C}^{N_2}$ are written as

$$\mathbf{a}_h(\theta_{k,\ell}^{\text{bs}}, \varphi_{k,\ell}^{\text{bs}}, d_1^{\text{bs}}) = \left[e^{-j\frac{2\pi}{\lambda}\left(\frac{N_1-1}{2}\right)d_1^{\text{bs}} \sin \theta_{k,\ell}^{\text{bs}} \cos \varphi_{k,\ell}^{\text{bs}}}, \dots, e^{+j\frac{2\pi}{\lambda}\left(\frac{N_1-1}{2}\right)d_1^{\text{bs}} \sin \theta_{k,\ell}^{\text{bs}} \cos \varphi_{k,\ell}^{\text{bs}}} \right]^T, \quad (8)$$

$$\mathbf{a}_v(\theta_{k,\ell}^{\text{bs}}, d_2^{\text{bs}}) = \left[e^{-j\frac{2\pi}{\lambda}\left(\frac{N_2-1}{2}\right)d_2^{\text{bs}} \cos \theta_{k,\ell}^{\text{bs}}}, \dots, e^{+j\frac{2\pi}{\lambda}\left(\frac{N_2-1}{2}\right)d_2^{\text{bs}} \cos \theta_{k,\ell}^{\text{bs}}} \right]^T. \quad (9)$$

The terrestrial channel matrix is $\mathbf{H} = [\mathbf{h}_1, \dots, \mathbf{h}_{K_t}] \in \mathbb{C}^{N \times K_t}$. As mentioned above, the channels from the terrestrial BS to the SUs are negligible because the SUs are located outside of the terrestrial BS coverage region.

3) *CSIT Estimation*: In this subsection, we explain the CSIT estimation. We assume that the perfect CSI is given at the users (including the SUs and the TUs) (i.e., perfect CSI at the receiver (CSIR)).³ Assuming time division duplex (TDD) that allow for channel reciprocity, each user sends a pilot sequence to estimate the uplink channel. Thanks to the reciprocity, the estimated uplink CSI is reused in design of downlink precoders. In this case, the CSIT estimation error is modeled based on the finite uplink pilot power and sequence length [27]. To incorporate the CSIT imperfection, we assume that CSIT is estimated via linear MMSE at both the LEO satellite and the terrestrial BS. Specifically, we denote the estimated channel vectors $\{\hat{\mathbf{g}}_u, \hat{\mathbf{z}}_k\} \in \mathbb{C}^M$ and $\hat{\mathbf{h}}_k \in \mathbb{C}^N$ as

$$\hat{\mathbf{g}}_u = \mathbf{g}_u - \mathbf{e}_u^{\text{sat}}, \quad \hat{\mathbf{z}}_k = \mathbf{z}_k - \mathbf{e}_k^{\text{sat}}, \quad \hat{\mathbf{h}}_k = \mathbf{h}_k - \mathbf{e}_k^{\text{bs}}, \quad (10)$$

where $\{\mathbf{q}_u^{\text{sat}}, \mathbf{e}_k^{\text{sat}}\} \in \mathbb{C}^M$ and $\mathbf{e}_k^{\text{bs}} \in \mathbb{C}^N$ are the CSIT estimation error vectors. The estimated error covariance matrices for each channel are given by a function of spatial covariance matrix, pilot length τ , and pilot transmission power p^{pi} , respectively:

$$\mathbf{Q}_u^{\text{sat}} = \mathbb{E}[\mathbf{q}_u^{\text{sat}}(\mathbf{q}_u^{\text{sat}})^H] = \mathbf{Q}_u - \mathbf{Q}_u \left(\mathbf{Q}_u + \frac{\sigma^2}{\tau p^{\text{pi}}} \mathbf{I}_M \right)^{-1} \mathbf{Q}_u, \quad (11)$$

$$\mathbf{\Phi}_k^{\text{sat}} = \mathbb{E}[\mathbf{e}_k^{\text{sat}}(\mathbf{e}_k^{\text{sat}})^H] = \mathbf{R}_k^{\text{sat}} - \mathbf{R}_k^{\text{sat}} \left(\mathbf{R}_k^{\text{sat}} + \frac{\sigma^2}{\tau p^{\text{pi}}} \mathbf{I}_M \right)^{-1} \mathbf{R}_k^{\text{sat}}, \quad (12)$$

$$\mathbf{\Phi}_k^{\text{bs}} = \mathbb{E}[\mathbf{e}_k^{\text{bs}}(\mathbf{e}_k^{\text{bs}})^H] = \mathbf{R}_k^{\text{bs}} - \mathbf{R}_k^{\text{bs}} \left(\mathbf{R}_k^{\text{bs}} + \frac{\sigma^2}{\tau p^{\text{pi}}} \mathbf{I}_N \right)^{-1} \mathbf{R}_k^{\text{bs}}, \quad (13)$$

where $\mathbf{Q}_u = \mathbb{E}[\mathbf{g}_u \mathbf{g}_u^H] \in \mathbb{C}^{M \times M}$, $\mathbf{R}_k^{\text{sat}} = \mathbb{E}[\mathbf{z}_k \mathbf{z}_k^H] \in \mathbb{C}^{M \times M}$ and $\mathbf{R}_k^{\text{bs}} = \mathbb{E}[\mathbf{h}_k \mathbf{h}_k^H] \in \mathbb{C}^{N \times N}$ are the channel spatial covariance matrices, and $\mathbf{I}_M \in \mathbb{C}^{M \times M}$, $\mathbf{I}_N \in \mathbb{C}^{N \times N}$ are the identity matrices. We assume that the channel spatial covariance matrices can be acquired at the LEO satellite and the terrestrial BS by exploiting the long-term channel information⁴ such as AoDs [20], [21]. We note that this CSIT error model is also applicable in high mobility scenarios, wherein CSI variation caused

³In practice, channel estimation errors can occur at receivers, too. For the sake of conciseness, this paper does not consider the case of imperfect CSIR. Incorporating imperfect CSIR is promising as future research.

⁴Due to high mobility of LEO satellites, however, even this long-term channel information can be frequently varying compared to that of terrestrial channels. Incorporating this into precoder design is interesting future work.

by mobility is represented by an auto-regressive function (i.e., first-order Gauss-Markov process) as in [28], [29].

Our model generalizes the previous satellite CSIT acquisition model used in [20]. In [20], two cases of CSIT acquisition were considered, instantaneous CSI (iCSI) and statistical CSI (sCSI). In iCSI, the CSIT is perfectly known at a LEO satellite, while in sCSI only the long-term channel covariance is available without any instantaneous channel knowledge. These are two extreme cases in our model, where the iCSI case corresponds to $\tau p^{\text{pi}} = \infty$ and the sCSI case corresponds to $\tau p^{\text{pi}} = 0$. In practice, it is more plausible that the CSIT is partially known at a satellite with some error depending on the used estimation methods. In this sense, our assumption is more general and realistic.

Lastly, we emphasize that our distributed precoding method is applicable in any CSIT estimation model. To be specific, the proposed method is developed provided that the CSIT estimation error can be calculated in transmitters as a function of the long-term channel covariance. We will provide a more detailed explanation of this in Section IV.

C. Signal Model

Satellite transmit signal: To effectively handle the interference of the LEO satellite without sharing CSIT, we exploit the RS strategy. To be specific, following the principle of 1-layer RS [30], the messages M_1, \dots, M_{K_s} intended to SUs are split into common parts and private parts, i.e., $M_u \rightarrow \{M_{c,u}, M_{p,u}\}$. The common parts $\{M_{c,1}, \dots, M_{c,K_s}\}$ are jointly combined and encoded into a common stream s_c . The private parts $M_{p,u}$ are independently encoded into the private stream $s_{p,u}$. For the common stream s_c , the corresponding codebook is shared with both the SUs in \mathcal{K}_s and the TUs in $\mathcal{K}_t^{\text{int}}$, who experience the interference from the LEO satellite. The codebook for the private stream $s_{p,u}$ is only given to SU u . Accordingly, s_c is decodable to the users in \mathcal{K}_s and $\mathcal{K}_t^{\text{int}}$, while $s_{p,u}$ is decodable only to SU u . Note that s_c and $s_{p,u}$ are drawn from independent Gaussian codebooks, i.e., $s_c, s_{p,u} \sim \mathcal{CN}(0, P_s)$ where P_s is the total transmit power of the LEO satellite.

At the LEO satellite, the common stream s_c and the private streams $s_{p,u}$ are linearly combined with the precoding vectors $\mathbf{f}_c \in \mathbb{C}^M$ and $\mathbf{f}_{p,u} \in \mathbb{C}^M$. Then the transmit signal vector of the LEO satellite $\mathbf{x}^{\text{sat}} \in \mathbb{C}^M$ is

$$\mathbf{x}^{\text{sat}} = \mathbf{f}_c s_c + \sum_{i=1}^{K_s} \mathbf{f}_{p,i} s_{p,i}. \quad (14)$$

We define $\mathbf{F} = [\mathbf{f}_c, \mathbf{f}_{p,1}, \dots, \mathbf{f}_{p,K_s}] \in \mathbb{C}^{M \times (K_s+1)}$ as the precoding matrix of the LEO satellite. For the transmit power constraint, we assume $\text{tr}(\mathbf{F}\mathbf{F}^H) \leq 1$, by which the total transmit power is constrained by P_s .

Terrestrial BS transmit signal: In the terrestrial BS, the unicast messages W_1, \dots, W_{K_t} are directly encoded into the streams m_1, \dots, m_{K_t} without RS. Each stream m_k is drawn from an independent Gaussian codebook, i.e., $m_k \sim \mathcal{CN}(0, P_t)$ where P_t is the total transmit power of the terrestrial BS. Then, the stream m_k are linearly combined with precoding vectors

$\mathbf{v}_k \in \mathbb{C}^N$. Accordingly, the transmit signal of the terrestrial BS $\mathbf{x}^{\text{bs}} \in \mathbb{C}^N$ is given by

$$\mathbf{x}^{\text{bs}} = \sum_{j=1}^{K_t} \mathbf{v}_j m_j, \quad (15)$$

The precoding matrix of the terrestrial BS is $\mathbf{V} = [\mathbf{v}_1, \dots, \mathbf{v}_{K_t}] \in \mathbb{C}^{N \times K_t}$ and the power constraint of terrestrial BS is $\text{tr}(\mathbf{V}\mathbf{V}^H) \leq 1$.

Received signal⁵ : The received signal at TU $k \in \mathcal{K}_t^{\text{int}}$ is

$$y_k = \mathbf{h}_k^H \sum_{j=1}^{K_t} \mathbf{v}_j m_j + \mathbf{z}_k^H \left(\mathbf{f}_c s_c + \sum_{i=1}^{K_s} \mathbf{f}_{p,i} s_{p,i} \right) + n_k, \quad (16)$$

where n_k is the additive white Gaussian noise (AWGN) with variance σ^2 and \mathbf{z}_k is the interference channel from the LEO satellite to TU k . If TU $k \notin \mathcal{K}_t^{\text{int}}$, $\mathbf{z}_k = \mathbf{0}$. The received signal of SU u is

$$y_u = \mathbf{g}_u^H \left(\mathbf{f}_c s_c + \sum_{i=1}^{K_s} \mathbf{f}_{p,i} s_{p,i} \right) + n_u, \quad (17)$$

where $n_u \sim \mathcal{CN}(0, \sigma^2)$ is AWGN. We note that there is no interference coming from the terrestrial BS to the SUs due to the limited coverage of a terrestrial BS.

D. Performance Metrics and Problem Formulation

1) Spectral Efficiency Characterization: Before formulating our main problem, we explain the decoding process in the considered RS strategy. Each user (including the SUs in \mathcal{K}_s and TUs in $\mathcal{K}_t^{\text{int}}$) first decodes the common stream s_c by treating all the other private streams as noise. Provided that the code rate of s_c is properly determined, it is guaranteed that the common stream is decoded without any error. After successfully decoding the common stream, each user removes the common stream from the received signal by using SIC. Then, the SUs and the TUs decode $s_{p,u}$ and m_k by using single-user decoding.

Given the perfect CSIT, the SINR of the common stream s_c at TU $k \in \mathcal{K}_t^{\text{int}}$ and the common stream s_c at SU u are respectively given by

$$\begin{aligned} \text{SINR}_{c,k} &= \frac{|\mathbf{z}_k^H \mathbf{f}_c|^2}{\sum_{j=1}^{K_t} |\mathbf{h}_k^H \mathbf{v}_j|^2 + \frac{P_s}{P_t} \sum_{i=1}^{K_s} |\mathbf{z}_k^H \mathbf{f}_{p,i}|^2 + \frac{\sigma^2}{P_t}}, \\ \text{SINR}_{c,u} &= \frac{|\mathbf{g}_u^H \mathbf{f}_c|^2}{\sum_{i=1}^{K_s} |\mathbf{g}_u^H \mathbf{f}_{p,i}|^2 + \frac{\sigma^2}{P_s}}. \end{aligned} \quad (18)$$

Note that, in $\text{SINR}_{c,u}$ of (18), there is no signal from the terrestrial BS due to the coverage restriction. The spectral efficiencies are denoted as $R_{c,k}(\mathbf{F}, \mathbf{V}) = \log_2(1 + \text{SINR}_{c,k})$ and $R_{c,u}(\mathbf{F}) = \log_2(1 + \text{SINR}_{c,u})$, respectively.

To guarantee that the users in \mathcal{K}_s and $\mathcal{K}_t^{\text{int}}$ can decode the common stream s_c , the code rate of the common stream should be determined as the minimum value of the spectral

⁵With compensation for Doppler and delay at each user, we assume perfect synchronization in both time and frequency between the terrestrial BS and TUs $\forall k \in \mathcal{K}_t$, as well as between the LEO satellite and both SUs $\forall u \in \mathcal{K}_s$ and TUs $\forall k \in \mathcal{K}_t^{\text{int}}$ [20], [21].

efficiencies among the users in $\mathcal{K}_t^{\text{int}}$ and \mathcal{K}_s ; thus, $R_c(\mathbf{F}, \mathbf{V}) = \min_{k \in \mathcal{K}_t^{\text{int}}, u \in \mathcal{K}_s} \{R_{c,k}(\mathbf{F}, \mathbf{V}), R_{c,u}(\mathbf{F})\}$. After cancelling s_c , TU $k \in \mathcal{K}_t$ and SU $u \in \mathcal{K}_s$ decode their desirable private streams, m_k and $s_{p,u}$. For TU k , the SINR of the private stream m_k is

$$\text{SINR}_{p,k} = \frac{|\mathbf{h}_k^H \mathbf{v}_k|^2}{\sum_{j=1, j \neq k}^{K_t} |\mathbf{h}_k^H \mathbf{v}_j|^2 + \frac{P_s}{P_t} \sum_{i=1}^{K_s} |\mathbf{z}_k^H \mathbf{f}_{p,i}|^2 + \frac{\sigma^2}{P_t}}. \quad (19)$$

The SINR of the private stream $s_{p,u}$ for SU u is

$$\text{SINR}_{p,u} = \frac{|\mathbf{g}_u^H \mathbf{f}_{p,u}|^2}{\sum_{i=1, i \neq u}^{K_s} |\mathbf{g}_u^H \mathbf{f}_{p,i}|^2 + \frac{\sigma^2}{P_s}}. \quad (20)$$

The spectral efficiencies of the private streams m_k and $s_{p,u}$ are respectively $R_{p,k}(\mathbf{F}, \mathbf{V}) = \log_2(1 + \text{SINR}_{p,k})$ and $R_{p,u}(\mathbf{F}) = \log_2(1 + \text{SINR}_{p,u})$.

Unfortunately, however, the spectral efficiencies $R_c(\mathbf{F}, \mathbf{V})$, $R_{p,k}(\mathbf{F}, \mathbf{V})$ and $R_{p,u}(\mathbf{F})$ cannot be computed under an imperfect CSIT setup. To address this, we derive a lower bound on the spectral efficiency. Specifically, we rewrite the received signals (16) and (17) with the estimated CSIT, i.e., (10), which yields

$$y_k = (\hat{\mathbf{h}}_k + \mathbf{e}_k^{\text{bs}})^H \sum_{j=1}^{K_t} \mathbf{v}_j m_j + (\hat{\mathbf{z}}_k + \mathbf{e}_k^{\text{sat}})^H \left(\mathbf{f}_c s_c + \sum_{i=1}^{K_s} \mathbf{f}_{p,i} s_{p,i} \right) + n_k, \quad (21)$$

$$y_u = (\hat{\mathbf{g}}_u^H + \mathbf{q}_u^{\text{sat}}) \left(\mathbf{f}_c s_c + \sum_{i=1}^{K_s} \mathbf{f}_{p,i} s_{p,i} \right) + n_u. \quad (22)$$

Applying a generalized mutual information technique [31], we treat the CSIT estimation error as independent Gaussian noise with appropriate moment matching. This makes a lower bound on $R_{c,k}(\mathbf{F}, \mathbf{V})$ as follows:

$$\begin{aligned} R_{c,k}(\mathbf{F}, \mathbf{V}) &\stackrel{(a)}{\geq} \mathbb{E} \left[\log_2 \left(1 + \frac{|\hat{\mathbf{z}}_k^H \mathbf{f}_c|^2}{\sum_{j=1}^{K_t} \{|\hat{\mathbf{h}}_k^H \mathbf{v}_j|^2 + \mathbf{v}_j^H \mathbf{F}_k^{\text{bs}} \mathbf{v}_j\} + \{|\mathbf{e}_k^{\text{sat}}|^2 + |\mathbf{e}_k^{\text{bs}}|^2\}} \right) \right] \\ &\stackrel{(b)}{\geq} \log_2 \left(1 + \frac{|\hat{\mathbf{z}}_k^H \mathbf{f}_c|^2}{I_{c,k}^U + I_{c,k}^C + \mathbf{f}_c^H \mathbb{E} [\mathbf{e}_k^{\text{sat}} (\mathbf{e}_k^{\text{sat}})^H] \mathbf{f}_c + \frac{\sigma^2}{P_t}} \right). \end{aligned} \quad (23)$$

In (a), the expectation is taken over the randomness associated with the CSIT estimation error $\{\mathbf{e}_k^{\text{bs}}, \mathbf{e}_k^{\text{sat}}\}$. We clarify that this lower bound technique was used in the prior work [30], [32]. (b) is obtained by applying Jensen's inequality where $I_{c,k}^U = \sum_{j=1}^{K_t} (|\hat{\mathbf{h}}_k^H \mathbf{v}_j|^2 + \mathbf{v}_j^H \mathbb{E}[\mathbf{e}_k^{\text{bs}} (\mathbf{e}_k^{\text{bs}})^H] \mathbf{v}_j)$ and $I_{c,k}^C = \frac{P_s}{P_t} \sum_{i=1}^{K_s} (|\hat{\mathbf{z}}_k^H \mathbf{f}_{p,i}|^2 + \mathbf{f}_{p,i}^H \mathbb{E}[\mathbf{e}_k^{\text{sat}} (\mathbf{e}_k^{\text{sat}})^H] \mathbf{f}_{p,i})$. By applying (12) and (13) to (23), the lower bound on $R_{c,k}(\mathbf{F}, \mathbf{V})$ is given by

$$\begin{aligned} R_{c,k}(\mathbf{F}, \mathbf{V}) &\geq \log_2 \left(1 + \left| \hat{\mathbf{z}}_k^H \mathbf{f}_c \right|^2 \right) \left/ \left\{ \begin{array}{l} \sum_{j=1}^{K_t} (|\hat{\mathbf{h}}_k^H \mathbf{v}_j|^2 + \mathbf{v}_j^H \mathbf{F}_k^{\text{bs}} \mathbf{v}_j) + \mathbf{f}_c^H \mathbf{F}_k^{\text{sat}} \mathbf{f}_c \\ + \frac{P_s}{P_t} \sum_{i=1}^{K_s} (|\hat{\mathbf{z}}_k^H \mathbf{f}_{p,i}|^2 + \mathbf{f}_{p,i}^H \mathbf{F}_k^{\text{sat}} \mathbf{f}_{p,i}) + \frac{\sigma^2}{P_t} \end{array} \right\} \right\} \\ &= \bar{R}_{c,k}(\mathbf{F}, \mathbf{V}). \end{aligned} \quad (24)$$

Since the error covariance matrices \mathbf{F}_k^{bs} and $\mathbf{F}_k^{\text{sat}}$ are assumed to be known at the LEO satellite, we are able to calculate (24)

as a closed-form. Likewise, a lower bound on the spectral efficiency of the common stream at SU u is acquired as follows.

$$\begin{aligned} R_{c,u}(\mathbf{F}) &\geq \log_2 \left(1 + \left| \hat{\mathbf{g}}_u^H \mathbf{f}_c \right|^2 \right) \left/ \left\{ \begin{array}{l} \sum_{i=1}^{K_s} (|\hat{\mathbf{g}}_u^H \mathbf{f}_{p,i}|^2 + \mathbf{f}_i^H \mathbf{F}_u^{\text{sat}} \mathbf{f}_{p,i}) \\ + \mathbf{f}_c^H \mathbf{F}_u^{\text{sat}} \mathbf{f}_c + \frac{\sigma^2}{P_s} \end{array} \right\} \right\} \\ &= \bar{R}_{c,u}(\mathbf{F}). \end{aligned} \quad (25)$$

We obtain a lower bound on the spectral efficiency of the private stream for TU k and SU u as

$$\begin{aligned} R_{p,k}(\mathbf{F}, \mathbf{V}) &\geq \log_2 \left(1 + \frac{|\hat{\mathbf{h}}_k^H \mathbf{v}_k|^2}{I_{p,k}^U + I_{p,k}^C + \mathbf{v}_k^H \mathbf{F}_k^{\text{bs}} \mathbf{v}_k + \frac{\sigma^2}{P_t}} \right) \\ &= \bar{R}_{p,k}(\mathbf{F}, \mathbf{V}), \end{aligned} \quad (26)$$

$$\begin{aligned} R_{p,u}(\mathbf{F}) &\geq \log_2 \left(1 + \left| \hat{\mathbf{g}}_u^H \mathbf{f}_{p,u} \right|^2 \right) \left/ \left\{ \begin{array}{l} \sum_{i=1, i \neq u}^{K_s} (|\hat{\mathbf{g}}_u^H \mathbf{f}_{p,i}|^2 + \mathbf{f}_{p,i}^H \mathbf{F}_u^{\text{sat}} \mathbf{f}_{p,i}) \\ + \mathbf{f}_{p,u}^H \mathbf{F}_u^{\text{sat}} \mathbf{f}_{p,u} + \frac{\sigma^2}{P_s} \end{array} \right\} \right\} \\ &= \bar{R}_{p,u}(\mathbf{F}), \end{aligned} \quad (27)$$

where $I_{p,k}^U = \sum_{j=1, j \neq k}^{K_t} (|\hat{\mathbf{h}}_k^H \mathbf{v}_j|^2 + \mathbf{v}_j^H \mathbf{F}_k^{\text{bs}} \mathbf{v}_j)$ and $I_{p,k}^C = \frac{P_s}{P_t} \sum_{i=1}^{K_s} (|\hat{\mathbf{z}}_k^H \mathbf{f}_{p,i}|^2 + \mathbf{f}_{p,i}^H \mathbf{F}_k^{\text{sat}} \mathbf{f}_{p,i})$ are represented by applying Jensen's inequality to the IUI term and ICI term for the private stream of TU k . With the obtained lower bounds on spectral efficiency, we formulate our main problem.

2) *Problem Formulation*: We formulate the following precoder design problem that aims to maximize a lower bound on the sum spectral efficiency with the RS strategy:

$$\mathcal{P}_1 : \underset{\{\mathbf{F}, \mathbf{V}\}}{\text{maximize}} \left[\begin{array}{l} \min_{k \in \mathcal{K}_t^{\text{int}}, u \in \mathcal{K}_s} \{\bar{R}_{c,k}(\mathbf{F}, \mathbf{V}), \bar{R}_{c,u}(\mathbf{F})\} \\ + \sum_{i=1}^{K_s} \bar{R}_{p,i}(\mathbf{F}) + \sum_{j=1}^{K_t} \bar{R}_{p,j}(\mathbf{F}, \mathbf{V}) \end{array} \right], \quad (28)$$

$$\begin{aligned} \text{subject to} \quad \text{tr}(\mathbf{F} \mathbf{F}^H) &= \|\mathbf{f}_c\|^2 + \sum_{i=1}^{K_s} \|\mathbf{f}_{p,i}\|^2 \leq 1, \\ \text{tr}(\mathbf{V} \mathbf{V}^H) &= \sum_{j=1}^{K_t} \|\mathbf{v}_j\|^2 \leq 1. \end{aligned} \quad (29)$$

We observe that solving \mathcal{P}_1 requires to share the estimated CSIT between the LEO satellite and the terrestrial BS, which corresponds to coordinated precoding design. This is not feasible in our distributed setup. Further, \mathcal{P}_1 is non-convex and also non-smooth, wherein finding a global optimal solution within polynomial time is infeasible. In the next section, we resolve these difficulties to develop a distributed method.

III. REFORMULATION TO DISTRIBUTED PROBLEM

In this section, we propose a novel distributed precoding design in which CSIT is not shared between the LEO satellite and terrestrial BS.

A. Representation to a Tractable Form

At first, we represent the optimization problem (28) into a tractable non-convex optimization problem expressed as a function of Rayleigh quotients. To this end, we stack all the precoding matrices \mathbf{F} and \mathbf{V} to rewrite them as higher-dimensional precoding vectors $\bar{\mathbf{f}} \in \mathbb{C}^{M(K_s+1)}$ and $\bar{\mathbf{v}} \in \mathbb{C}^{N K_t}$, denoted as,

$$\bar{\mathbf{f}} = \left[\mathbf{f}_c^T, \mathbf{f}_{p,1}^T, \dots, \mathbf{f}_{p,K_s}^T \right]^T, \quad \bar{\mathbf{v}} = \left[\mathbf{v}_1^T, \dots, \mathbf{v}_{K_t}^T \right]^T. \quad (30)$$

We also define a unit vector whose the k -th element is 1 and the rest of the elements are zero as $\mathbf{u}_k = [0, \dots, 1, \dots, 0]^\top \in \mathbb{R}^{K_t}$, and a unit vector whose the $(u+1)$ -th element 1 and the rest of the elements zero as $\mathbf{w}_u = [0, 0, \dots, 1, \dots, 0]^\top \in \mathbb{R}^{(K_s+1)}$.

With (30), the spectral efficiency for the common stream of TU k (24) is expressed by

$$\bar{R}_{c,k}(\bar{\mathbf{f}}, \bar{\mathbf{v}}) = \log_2 \left(\frac{\bar{\mathbf{v}}^\text{H} \mathbf{U}_{c,k}^{\text{bs}} \bar{\mathbf{v}} + \bar{\mathbf{f}}^\text{H} (\mathbf{S}_{c,k}^{\text{bs}} + \mathbf{C}_{c,k}^{\text{bs}}) \bar{\mathbf{f}}}{\bar{\mathbf{v}}^\text{H} \mathbf{U}_{c,k}^{\text{bs}} \bar{\mathbf{v}} + \bar{\mathbf{f}}^\text{H} \mathbf{C}_{c,k}^{\text{bs}} \bar{\mathbf{f}}} \right), \quad (31)$$

where $\mathbf{S}_{c,k}^{\text{bs}} \in \mathbb{C}^{M(K_s+1) \times M(K_s+1)}$, $\mathbf{U}_{c,k}^{\text{bs}} \in \mathbb{C}^{NK_t \times NK_t}$ and $\mathbf{C}_{c,k}^{\text{bs}} \in \mathbb{C}^{M(K_s+1) \times M(K_s+1)}$ are defined as

$$\mathbf{S}_{c,k}^{\text{bs}} = \mathbf{w}_0 \mathbf{w}_0^\text{H} \otimes \hat{\mathbf{z}}_k \hat{\mathbf{z}}_k^\text{H}, \quad (32)$$

$$\mathbf{U}_{c,k}^{\text{bs}} = \mathbf{I}_{K_t} \otimes (\hat{\mathbf{h}}_k \hat{\mathbf{h}}_k^\text{H} + \Phi_k^{\text{bs}}) + \frac{\sigma^2}{P_t} \mathbf{I}_{NK_t}, \quad (33)$$

$$\mathbf{C}_{c,k}^{\text{bs}} = \mathbf{I}_{K_s+1} \otimes (\hat{\mathbf{z}}_k \hat{\mathbf{z}}_k^\text{H} + \Phi_k^{\text{sat}}) - \mathbf{S}_{c,k}^{\text{bs}}. \quad (34)$$

We also write the spectral efficiency for the common stream of SU u (25) as

$$\bar{R}_{c,u}(\bar{\mathbf{f}}) = \log_2 \left(\frac{\bar{\mathbf{f}}^\text{H} (\mathbf{S}_{c,u}^{\text{sat}} + \mathbf{U}_{c,u}^{\text{sat}}) \bar{\mathbf{f}}}{\bar{\mathbf{f}}^\text{H} \mathbf{U}_{c,u}^{\text{sat}} \bar{\mathbf{f}}} \right), \quad (35)$$

where $\mathbf{S}_{c,u}^{\text{sat}} \in \mathbb{C}^{M(K_s+1) \times M(K_s+1)}$, $\mathbf{U}_{c,u}^{\text{sat}} \in \mathbb{C}^{M(K_s+1) \times M(K_s+1)}$ are given by

$$\mathbf{S}_{c,u}^{\text{sat}} = \mathbf{w}_0 \mathbf{w}_0^\text{H} \otimes \hat{\mathbf{g}}_u \hat{\mathbf{g}}_u^\text{H}, \quad (36)$$

$$\mathbf{U}_{c,u}^{\text{sat}} = \mathbf{I}_{K_s+1} \otimes (\hat{\mathbf{g}}_u \hat{\mathbf{g}}_u^\text{H} + \Psi_u^{\text{sat}}) + \frac{\sigma^2}{P_s} \mathbf{I}_{M(K_s+1)} - \mathbf{S}_{c,u}^{\text{sat}}. \quad (37)$$

Similar to this, the spectral efficiency for the private stream of TU k (26) is also written by

$$\bar{R}_{p,k}(\bar{\mathbf{f}}, \bar{\mathbf{v}}) = \log_2 \left(\frac{\bar{\mathbf{v}}^\text{H} (\mathbf{S}_{p,k}^{\text{bs}} + \mathbf{U}_{p,k}^{\text{bs}}) \bar{\mathbf{v}} + \bar{\mathbf{f}}^\text{H} \mathbf{C}_{p,k}^{\text{bs}} \bar{\mathbf{f}}}{\bar{\mathbf{v}}^\text{H} \mathbf{U}_{p,k}^{\text{bs}} \bar{\mathbf{v}} + \bar{\mathbf{f}}^\text{H} \mathbf{C}_{p,k}^{\text{bs}} \bar{\mathbf{f}}} \right), \quad (38)$$

where $\mathbf{S}_{p,k}^{\text{bs}} \in \mathbb{C}^{NK_t \times NK_t}$, $\mathbf{U}_{p,k}^{\text{bs}} \in \mathbb{C}^{NK_t \times NK_t}$ and $\mathbf{C}_{p,k}^{\text{bs}} \in \mathbb{C}^{M(K_s+1) \times M(K_s+1)}$ are

$$\mathbf{S}_{p,k}^{\text{bs}} = \mathbf{u}_k \mathbf{u}_k^\text{H} \otimes \hat{\mathbf{h}}_k \hat{\mathbf{h}}_k^\text{H}, \quad (39)$$

$$\mathbf{U}_{p,k}^{\text{bs}} = \mathbf{I}_{K_t} \otimes (\hat{\mathbf{h}}_k \hat{\mathbf{h}}_k^\text{H} + \Phi_k^{\text{bs}}) + \frac{\sigma^2}{P_t} \mathbf{I}_{NK_t} - \mathbf{S}_{p,k}^{\text{bs}}, \quad (40)$$

$$\mathbf{C}_{p,k}^{\text{bs}} = \mathbf{I}_{K_s+1} \otimes \frac{P_s}{P_t} (\hat{\mathbf{z}}_k \hat{\mathbf{z}}_k^\text{H} + \Phi_k^{\text{sat}}) - \mathbf{w}_0 \mathbf{w}_0^\text{H} \otimes (\hat{\mathbf{z}}_k \hat{\mathbf{z}}_k^\text{H} + \Phi_k^{\text{sat}}). \quad (41)$$

Next, we present the spectral efficiency for the private stream of SU u (27) as

$$\bar{R}_{p,u}(\bar{\mathbf{f}}) = \log_2 \left(\frac{\bar{\mathbf{f}}^\text{H} (\mathbf{S}_{p,u}^{\text{sat}} + \mathbf{U}_{p,u}^{\text{sat}}) \bar{\mathbf{f}}}{\bar{\mathbf{f}}^\text{H} \mathbf{U}_{p,u}^{\text{sat}} \bar{\mathbf{f}}} \right), \quad (42)$$

where $\mathbf{S}_{p,u}^{\text{sat}}$ and $\mathbf{U}_{p,u}^{\text{sat}}$ are given by

$$\mathbf{S}_{p,u}^{\text{sat}} = \mathbf{w}_u \mathbf{w}_u^\text{H} \otimes \hat{\mathbf{g}}_u \hat{\mathbf{g}}_u^\text{H} \in \mathbb{C}^{M(K_s+1) \times M(K_s+1)}, \quad (43)$$

$$\mathbf{U}_{p,u}^{\text{sat}} = \text{Blkd} [0, \mathbf{I}_{K_s}] \otimes (\hat{\mathbf{g}}_u \hat{\mathbf{g}}_u^\text{H} + \Psi_u^{\text{sat}}) + \frac{\sigma^2}{P_s} \text{Blkd} [\mathbf{0}_M, \mathbf{I}_{MK_s}] - \mathbf{S}_{p,u}^{\text{sat}} \in \mathbb{C}^{M(K_s+1) \times M(K_s+1)}. \quad (44)$$

Here, $\mathbf{0}_M \in \mathbb{C}^{M \times M}$ is the null matrix and $\text{Blkd} [\mathbf{0}_M, \mathbf{I}_{MK_s}] \in \mathbb{C}^{M(K_s+1) \times M(K_s+1)}$ is a block-diagonal matrix concatenating $\mathbf{0}_M, \mathbf{I}_{MK_s}$. In (31), (35), (38) and (42), we assume that the higher-dimensional precoding vectors $\bar{\mathbf{f}}$ and $\bar{\mathbf{v}}$ satisfy the transmit power constraint with equality, i.e., $\|\bar{\mathbf{f}}\|^2 = 1$ and $\|\bar{\mathbf{v}}\|^2 = 1$. Note that this assumption does not affect the optimality [30]. Using our representation, the sum spectral efficiency in (28) is expressed as

$$\begin{aligned} \bar{R}_{\text{sum}}(\bar{\mathbf{f}}, \bar{\mathbf{v}}) &= \min_{k \in \mathcal{K}_t^{\text{int}}, u \in \mathcal{K}_s} \{ \bar{R}_{c,k}(\bar{\mathbf{f}}, \bar{\mathbf{v}}), \bar{R}_{c,u}(\bar{\mathbf{f}}) \} \\ &+ \sum_{i=1}^{K_s} \bar{R}_{p,i}(\bar{\mathbf{f}}) + \sum_{j=1}^{K_t} \bar{R}_{p,j}(\bar{\mathbf{f}}, \bar{\mathbf{v}}). \end{aligned} \quad (45)$$

However, the sum spectral efficiency (45) cannot be solved in a distributed fashion yet because the LEO satellite precoding vector $\bar{\mathbf{f}}$ and the terrestrial BS precoding vector $\bar{\mathbf{v}}$ are entangled in $\bar{R}_{c,k}(\bar{\mathbf{f}}, \bar{\mathbf{v}})$ and $\bar{R}_{p,k}(\bar{\mathbf{f}}, \bar{\mathbf{v}})$. In the following subsection, we explain how to decouple $\bar{R}_{c,k}(\bar{\mathbf{f}}, \bar{\mathbf{v}})$ and $\bar{R}_{p,k}(\bar{\mathbf{f}}, \bar{\mathbf{v}})$; so that the LEO satellite and the terrestrial BS individually devise its precoding vector without sharing CSIT.

B. Transformation to Distributed Forms

Private stream spectral efficiency decoupling: We first decouple $\bar{R}_{p,k}(\bar{\mathbf{f}}, \bar{\mathbf{v}})$ defined in (38). A key challenge in decoupling of $\bar{R}_{p,k}(\bar{\mathbf{f}}, \bar{\mathbf{v}})$ is that the IUI term $\bar{\mathbf{v}}^\text{H} \mathbf{U}_{p,k}^{\text{bs}} \bar{\mathbf{v}}$, a function of $\bar{\mathbf{v}}$, and the ICI term $\bar{\mathbf{f}}^\text{H} \mathbf{C}_{p,k}^{\text{bs}} \bar{\mathbf{f}}$, a function of $\bar{\mathbf{f}}$, coexist in the numerator and the denominator as shown in (38). To resolve this, we consider the ergodic spectral efficiency where the expectation is taken over the randomness associated with the imperfect knowledge of the channel fading process: $\mathbb{E}_{\{\hat{\mathbf{h}}_k, \hat{\mathbf{z}}_k\}} [\bar{R}_{p,k}(\bar{\mathbf{f}}, \bar{\mathbf{v}})]$. For simplicity, we drop the notation of $\{\hat{\mathbf{h}}_k, \hat{\mathbf{z}}_k\}$ from the expectation. Assuming a high SNR regime, we approximate

$$\begin{aligned} \mathbb{E} [\bar{R}_{p,k}(\bar{\mathbf{f}}, \bar{\mathbf{v}})] &\stackrel{(a)}{\approx} \mathbb{E} \left[\log_2 \left(\frac{\bar{\mathbf{v}}^\text{H} \mathbf{S}_{p,k}^{\text{bs}} \bar{\mathbf{v}}}{\bar{\mathbf{v}}^\text{H} \mathbf{U}_{p,k}^{\text{bs}} \bar{\mathbf{v}} + \bar{\mathbf{f}}^\text{H} \mathbf{C}_{p,k}^{\text{bs}} \bar{\mathbf{f}}} \right) \right] \\ &\stackrel{(b)}{\geq} \mathbb{E} \left[\log_2 \left(\frac{\bar{\mathbf{v}}^\text{H} \mathbf{S}_{p,k}^{\text{bs}} \bar{\mathbf{v}}}{\mathbb{E} [\bar{\mathbf{v}}^\text{H} \mathbf{U}_{p,k}^{\text{bs}} \bar{\mathbf{v}}] + \bar{\mathbf{f}}^\text{H} \mathbf{C}_{p,k}^{\text{bs}} \bar{\mathbf{f}}} \right) \right] \\ &= \mathbb{E} \left[\log_2 \left(\frac{\bar{\mathbf{v}}^\text{H} \mathbf{S}_{p,k}^{\text{bs}} \bar{\mathbf{v}}}{\bar{\mathbf{f}}^\text{H} (\mathbf{C}_{p,k}^{\text{bs}} + \epsilon_k \mathbf{I}_{M(K_s+1)}) \bar{\mathbf{f}}} \right) \right], \end{aligned} \quad (46)$$

where (a) comes from the high SNR assumption and (b) follows Jensen's inequality. As observed in (b), by averaging the IUI term, it becomes a constant, i.e., $\mathbb{E} [\bar{\mathbf{v}}^\text{H} \mathbf{U}_{p,k}^{\text{bs}} \bar{\mathbf{v}}] = \epsilon_k$, we disentangle the $\bar{\mathbf{f}}$ -related term and the $\bar{\mathbf{v}}$ -related term into the numerator and the denominator in (46). With (46), by rearranging the ergodic sum spectral efficiency of the private streams, we obtain (47) as shown at the top of the next page. In (47), (a) follows from the high SNR approximation and Jensen's inequality. In the above derivation, it is noted in (b) that the ICI term $\bar{\mathbf{f}}^\text{H} (\mathbf{C}_{p,k}^{\text{bs}} + \epsilon_k \mathbf{I}_{M(K_s+1)}) \bar{\mathbf{f}}$ in $\bar{R}_{p,k}(\bar{\mathbf{f}}, \bar{\mathbf{v}})$ comes out as a product of the leakage interference $\left\{ \prod_{j=1}^{K_t} \bar{\mathbf{f}}^\text{H} (\mathbf{C}_{p,j}^{\text{bs}} + \epsilon_j \mathbf{I}_{M(K_s+1)}) \bar{\mathbf{f}} \right\}^{\frac{1}{K_s}}$, which is a function of only $\bar{\mathbf{f}}$. Thanks to this, we integrate this leakage interference

$$\begin{aligned}
& \sum_{i=1}^{K_s} \mathbb{E} [\bar{R}_{p,i}(\bar{\mathbf{f}})] + \sum_{j=1}^{K_t} \mathbb{E} [\bar{R}_{p,j}(\bar{\mathbf{f}}, \bar{\mathbf{v}})] \stackrel{(a)}{\geq} \sum_{i=1}^{K_s} \mathbb{E} \left[\log_2 \left(\frac{\bar{\mathbf{f}}^H (\mathbf{S}_{p,i}^{\text{sat}} + \mathbf{U}_{p,i}^{\text{sat}}) \bar{\mathbf{f}}}{\bar{\mathbf{f}}^H \mathbf{U}_{p,i}^{\text{sat}} \bar{\mathbf{f}}} \right) \right] + \sum_{j=1}^{K_t} \mathbb{E} \left[\log_2 \left(\frac{\bar{\mathbf{v}}^H \mathbf{S}_{p,j}^{\text{bs}} \bar{\mathbf{v}}}{\bar{\mathbf{f}}^H (\mathbf{C}_{p,j}^{\text{bs}} + \epsilon_j \mathbf{I}_{M(K_s+1)}) \bar{\mathbf{f}}} \right) \right] \\
& = \mathbb{E} \left[\log_2 \left(\prod_{i=1}^{K_s} \frac{\bar{\mathbf{f}}^H (\mathbf{S}_{p,i}^{\text{sat}} + \mathbf{U}_{p,i}^{\text{sat}}) \bar{\mathbf{f}}}{\bar{\mathbf{f}}^H \mathbf{U}_{p,i}^{\text{sat}} \bar{\mathbf{f}}} \prod_{j=1}^{K_t} \frac{\bar{\mathbf{v}}^H \mathbf{S}_{p,j}^{\text{bs}} \bar{\mathbf{v}}}{\bar{\mathbf{f}}^H (\mathbf{C}_{p,j}^{\text{bs}} + \epsilon_j \mathbf{I}_{M(K_s+1)}) \bar{\mathbf{f}}} \right) \right] \stackrel{(b)}{=} \mathbb{E} \left[\log_2 \left(\frac{\prod_{i=1}^{K_s} \bar{\mathbf{f}}^H (\mathbf{S}_{p,i}^{\text{sat}} + \mathbf{U}_{p,i}^{\text{sat}}) \bar{\mathbf{f}}}{\prod_{i=1}^{K_s} \bar{\mathbf{f}}^H \mathbf{U}_{p,i}^{\text{sat}} \bar{\mathbf{f}} \prod_{j=1}^{K_t} \bar{\mathbf{f}}^H (\mathbf{C}_{p,j}^{\text{bs}} + \epsilon_j \mathbf{I}_{M(K_s+1)}) \bar{\mathbf{f}}} \prod_{j=1}^{K_t} \bar{\mathbf{v}}^H \mathbf{S}_{p,j}^{\text{bs}} \bar{\mathbf{v}} \right) \right] \\
& = \sum_{i=1}^{K_s} \mathbb{E} \left[\log_2 \left(\frac{\bar{\mathbf{f}}^H (\mathbf{S}_{p,i}^{\text{sat}} + \mathbf{U}_{p,i}^{\text{sat}}) \bar{\mathbf{f}}}{\bar{\mathbf{f}}^H \mathbf{U}_{p,i}^{\text{sat}} \bar{\mathbf{f}} \cdot \left\{ \prod_{j=1}^{K_t} \bar{\mathbf{f}}^H (\mathbf{C}_{p,j}^{\text{bs}} + \epsilon_j \mathbf{I}_{M(K_s+1)}) \bar{\mathbf{f}} \right\}^{\frac{1}{K_s}}} \right) \right] + \underbrace{\sum_{j=1}^{K_t} \mathbb{E} \left[\log_2 \left(\bar{\mathbf{v}}^H \mathbf{S}_{p,j}^{\text{bs}} \bar{\mathbf{v}} \right) \right]}_{(c)}, \tag{47}
\end{aligned}$$

term into $\bar{R}_{p,i}(\bar{\mathbf{f}})$ as shown in (b). In (47), the private stream spectral efficiency is reshaped into two decoupled terms, wherein the first term is a function of $\bar{\mathbf{f}}$ and the second term is a function of $\bar{\mathbf{v}}$. This enables to tackle the problem in a distributed fashion. Nonetheless, we observe in (c) that the IUI term vanishes since we take average and pull out from $\bar{R}_{p,k}(\bar{\mathbf{f}}, \bar{\mathbf{v}})$ for decoupling (46). To compensate this, we restore the vanished IUI term in (c) as follows:

$$\begin{aligned}
\sum_{j=1}^{K_t} \mathbb{E} \left[\log_2 \left(\bar{\mathbf{v}}^H \mathbf{S}_{p,j}^{\text{bs}} \bar{\mathbf{v}} \right) \right] &= \mathbb{E} \left[\log_2 \left(\prod_{j=1}^{K_t} \frac{\bar{\mathbf{v}}^H \mathbf{S}_{p,j}^{\text{bs}} \bar{\mathbf{v}} \cdot \bar{\mathbf{v}}^H \mathbf{U}_{p,j}^{\text{bs}} \bar{\mathbf{v}}}{\bar{\mathbf{v}}^H \mathbf{U}_{p,j}^{\text{bs}} \bar{\mathbf{v}}} \right) \right] \\
&= \mathbb{E} \left[\log_2 \left(\prod_{j=1}^{K_t} \frac{\bar{\mathbf{v}}^H \mathbf{S}_{p,j}^{\text{bs}} \bar{\mathbf{v}}}{\bar{\mathbf{v}}^H \mathbf{U}_{p,j}^{\text{bs}} \bar{\mathbf{v}}} \right) \right] + \hat{\epsilon}, \tag{48}
\end{aligned}$$

where $\hat{\epsilon} = \mathbb{E} [\sum_{j=1}^{K_t} \log_2 (\bar{\mathbf{v}}^H \mathbf{U}_{p,j}^{\text{bs}} \bar{\mathbf{v}})]$. Inserting $\hat{\epsilon}$ into the $\bar{\mathbf{f}}$ related term, we get

$$\begin{aligned}
& \sum_{i=1}^{K_s} \mathbb{E} [\bar{R}_{p,i}(\bar{\mathbf{f}})] + \sum_{j=1}^{K_t} \mathbb{E} [\bar{R}_{p,j}(\bar{\mathbf{f}}, \bar{\mathbf{v}})] \\
& \gtrsim \sum_{i=1}^{K_s} \mathbb{E} [\bar{\Gamma}_{p,i}(\bar{\mathbf{f}})] + \sum_{j=1}^{K_t} \mathbb{E} [\bar{\Gamma}_{p,j}(\bar{\mathbf{v}})], \tag{49}
\end{aligned}$$

where

$$\begin{aligned}
& \mathbb{E} [\bar{\Gamma}_{p,u}(\bar{\mathbf{f}})] \\
& = \mathbb{E} \left[\log_2 \left(\frac{2^{\frac{\hat{\epsilon}}{K_s}} \cdot \bar{\mathbf{f}}^H (\mathbf{S}_{p,u}^{\text{sat}} + \mathbf{U}_{p,u}^{\text{sat}}) \bar{\mathbf{f}}}{\bar{\mathbf{f}}^H \mathbf{U}_{p,u}^{\text{sat}} \bar{\mathbf{f}} \cdot \left\{ \prod_{j=1}^{K_t} \bar{\mathbf{f}}^H (\mathbf{C}_{p,j}^{\text{bs}} + \epsilon_j \mathbf{I}_{M(K_s+1)}) \bar{\mathbf{f}} \right\}^{\frac{1}{K_s}}} \right) \right], \tag{50}
\end{aligned}$$

$$\mathbb{E} [\bar{\Gamma}_{p,k}(\bar{\mathbf{v}})] = \mathbb{E} \left[\log_2 \left(\bar{\mathbf{v}}^H \mathbf{S}_{p,k}^{\text{bs}} \bar{\mathbf{v}} \right) \right]. \tag{51}$$

It can be seen that $\bar{\Gamma}_{p,u}(\bar{\mathbf{f}})$ and $\bar{\Gamma}_{p,k}(\bar{\mathbf{v}})$ are functions of only $\bar{\mathbf{f}}$ and $\bar{\mathbf{v}}$ respectively, thus each can be maximized in a distributed fashion without CSIT sharing. Note that the LEO satellite is required to have knowledge on ϵ_k and $\hat{\epsilon}$ to maximize $\bar{\Gamma}_{p,u}(\bar{\mathbf{f}})$. We emphasize that ϵ_k and $\hat{\epsilon}$ are constants that does not vary over channels. This is because ϵ_k and $\hat{\epsilon}$ are obtained by averaging channel realizations and designed precoders. For this reason, it is very easy to deliver these values to the LEO

satellite, for instance by embedding into the control channels without incurring much overheads.

Common stream spectral efficiency decoupling: We reform the common stream spectral efficiency $\bar{R}_{c,k}(\bar{\mathbf{f}}, \bar{\mathbf{v}})$ in (31) by a distributed way. A critical obstacle to decouple $\bar{R}_{c,k}(\bar{\mathbf{f}}, \bar{\mathbf{v}})$ is that $\bar{\mathbf{v}}^H \mathbf{U}_{c,k}^{\text{bs}} \bar{\mathbf{v}}$ exists in the denominator of $\bar{R}_{c,k}(\bar{\mathbf{f}}, \bar{\mathbf{v}})$. To resolve this, we consider the ergodic spectral efficiency of common stream for TU k and its lower bound as follows:

$$\begin{aligned}
\mathbb{E} [\bar{R}_{c,k}(\bar{\mathbf{f}}, \bar{\mathbf{v}})] &= \mathbb{E} \left[\log_2 \left(1 + \frac{\bar{\mathbf{f}}^H \mathbf{S}_{c,k}^{\text{bs}} \bar{\mathbf{f}}}{\bar{\mathbf{v}}^H \mathbf{U}_{c,k}^{\text{bs}} \bar{\mathbf{v}} + \bar{\mathbf{f}}^H \mathbf{C}_{c,k}^{\text{bs}} \bar{\mathbf{f}}} \right) \right] \\
&\stackrel{(a)}{\geq} \mathbb{E} \left[\log_2 \left(1 + \frac{\bar{\mathbf{f}}^H \mathbf{S}_{c,k}^{\text{bs}} \bar{\mathbf{f}}}{\mathbb{E} [\bar{\mathbf{v}}^H \mathbf{U}_{c,k}^{\text{bs}} \bar{\mathbf{v}}] + \bar{\mathbf{f}}^H \mathbf{C}_{c,k}^{\text{bs}} \bar{\mathbf{f}}} \right) \right], \tag{52}
\end{aligned}$$

where the expectation is taken over the randomness associated with the imperfect knowledge of the channel fading process. (a) is the lower bound with Jensen's inequality applied. In (52), by averaging the IUI term, it becomes a constant, i.e., $\mathbb{E} [\bar{\mathbf{v}}^H \mathbf{U}_{c,k}^{\text{bs}} \bar{\mathbf{v}}] = \omega_k$, we can transform $\bar{R}_{c,k}(\bar{\mathbf{f}}, \bar{\mathbf{v}})$, which is a joint function of $\bar{\mathbf{f}}$ and $\bar{\mathbf{v}}$, into $\bar{\Gamma}_{c,k}(\bar{\mathbf{f}})$, which is a single function of $\bar{\mathbf{f}}$:

$$\begin{aligned}
\mathbb{E} [\bar{R}_{c,k}(\bar{\mathbf{f}}, \bar{\mathbf{v}})] &\geq \mathbb{E} [\bar{\Gamma}_{c,k}(\bar{\mathbf{f}})] \\
&= \mathbb{E} \left[\log_2 \left(\frac{\bar{\mathbf{f}}^H (\mathbf{S}_{c,k}^{\text{bs}} + \mathbf{C}_{c,k}^{\text{bs}} + \omega_k \mathbf{I}_{M(K_s+1)}) \bar{\mathbf{f}}}{\bar{\mathbf{f}}^H (\mathbf{C}_{c,k}^{\text{bs}} + \omega_k \mathbf{I}_{M(K_s+1)}) \bar{\mathbf{f}}} \right) \right]. \tag{53}
\end{aligned}$$

By doing this, provided that ω_k is known to the LEO satellite, it is feasible to maximize the common stream spectral efficiency at the LEO satellite without sharing CSIT. Similar to ϵ_k and $\hat{\epsilon}$, ω_k is a constant; thereby it is relative effortless to deliver ω_k to the LEO satellite.

Distributed problem formulation: Up to this point, we transform $\mathbb{E} [\bar{R}_{c,k}(\bar{\mathbf{f}}, \bar{\mathbf{v}})]$ and $\mathbb{E} [\bar{R}_{p,k}(\bar{\mathbf{f}}, \bar{\mathbf{v}})]$ to $\mathbb{E} [\bar{\Gamma}_{c,k}(\bar{\mathbf{f}})]$ and $\mathbb{E} [\bar{\Gamma}_{p,k}(\bar{\mathbf{v}})]$, wherein distributed precoding optimization is feasible because of our spectral efficiency decoupling. Based on this, we reformulate our main problem \mathcal{P}_1 in (28). We first recall that the expectation considered in the ergodic spectral efficiency (49) and (53) is associated with the randomness of the imperfect knowledge on channel fading process, i.e., $\mathbb{E} [\hat{\mathbf{h}}_k, \hat{\mathbf{g}}_u, \hat{\mathbf{z}}_k] [\cdot]$. Since the LEO satellite and the terrestrial BS are assumed to be aware of estimated CSIT $\hat{\mathbf{g}}_u, \hat{\mathbf{z}}_k$, (the satellite channel) and $\hat{\mathbf{h}}_k$ (the terrestrial channel), maximizing the ergodic spectral efficiency is equivalent to maximizing the

spectral efficiency by using the estimated CSIT given per each channel block. For this reason, we can omit $\mathbb{E}[\cdot]$ in (49) and (53). We note that the same concept was presented in [30], [33]. Consequently, we formulate the distributed precoding optimization problem as

$$\mathcal{P}_2 : \underset{\bar{\mathbf{f}}, \bar{\mathbf{v}}}{\text{maximize}} \left[\min_{k \in \mathcal{K}_t^{\text{int}}, u \in \mathcal{K}_s} \{ \bar{\Gamma}_{c,k}(\bar{\mathbf{f}}), \bar{R}_{c,u}(\bar{\mathbf{f}}) \} \right], \quad (54)$$

$$\text{subject to } \|\bar{\mathbf{f}}\|^2 = 1, \|\bar{\mathbf{v}}\|^2 = 1. \quad (55)$$

It is noteworthy that in \mathcal{P}_2 , all the spectral efficiencies in the objective function are exclusively determined by $\bar{\mathbf{f}}$ and $\bar{\mathbf{v}}$ respectively. This eliminates the necessity of CSIT sharing in solving \mathcal{P}_2 . Furthermore, the precoding vectors $\bar{\mathbf{f}}, \bar{\mathbf{v}}$ respectively can be normalized by dividing the numerator and denominator of Rayleigh quotient with $\|\bar{\mathbf{f}}\|^2$ and $\|\bar{\mathbf{v}}\|^2$, without affecting the objective function. Thanks to this reason, the constraint (55) can be omitted in (54).

Remark 1. (Interference report mechanism) To solve \mathcal{P}_2 , it is required to report $\epsilon_k, \hat{\epsilon}$, and ω_k to the satellite. Depending on reporting frequencies, we consider three following cases.

i) **Average report mechanism:** In this case, TUs report $\epsilon_k, \hat{\epsilon}$, and ω_k to the LEO satellite once. To this end, we first generate $\mathbf{U}_{p,k}^{\text{bs}}$ and $\mathbf{U}_{c,k}^{\text{bs}}$ by a Monte-Carlo fashion. Then, we design $\bar{\mathbf{v}}$ accordingly and calculate $\mathbb{E}[\bar{\mathbf{v}}^H \mathbf{U}_{p,k}^{\text{bs}} \bar{\mathbf{v}}] = \epsilon_k$ and $\mathbb{E}[\bar{\mathbf{v}}^H \mathbf{U}_{c,k}^{\text{bs}} \bar{\mathbf{v}}] = \omega_k$ by averaging the results. Finally, these averaged values are reported to the LEO satellite. This method corresponds to a case that we mainly explain in Section III.

ii) **Instantaneous report mechanism:** In this case, the report is carried per every channel coherence block. Specifically, in the Average report mechanism, the performance loss is inevitable since the precoding vector $\bar{\mathbf{f}}$ cannot reflect the instantaneous interference environment; yet only exploits the averaged value. To compensate this, we report the instantaneous received signal power $\bar{\mathbf{v}}^H \mathbf{U}_{c,k}^{\text{bs}} \bar{\mathbf{v}}$ to the LEO satellite. Since the instantaneous received signal power $\bar{\mathbf{v}}^H \mathbf{U}_{c,k}^{\text{bs}} \bar{\mathbf{v}}$ is determined depending on the instantaneous channel realization, the TUs are required to deliver it per every channel block, which consumes more overheads compared to the Average report mechanism.

iii) **Zero report mechanism:** In this case, we never report by setting $\epsilon_k = 0$ and $\omega_k = 0$. While this mechanism has an advantage of not consuming overheads, it comes with a drawback of not managing interference effectively, leading to some performance degradation.

In Section V, we will numerically compare the spectral efficiency performances for the three report mechanism.

IV. PRECODER OPTIMIZATION WITH GENERALIZED POWER ITERATION

In this section, we propose a GPI-based algorithm to solve \mathcal{P}_2 .

A. LSE Approximation

One challenge in solving \mathcal{P}_2 is the non-smoothness of the minimum function $\min_{k \in \mathcal{K}_t^{\text{int}}, u \in \mathcal{K}_s} \{ \bar{\Gamma}_{c,k}(\bar{\mathbf{f}}), \bar{R}_{c,u}(\bar{\mathbf{f}}) \}$. To resolve this, we first approximate the non-smooth minimum

function in (54) as a smooth function using the LSE technique [34]. Applying the LSE technique, the minimum function in (54) is approximated as follows

$$\begin{aligned} & \min_{k \in \mathcal{K}_t^{\text{int}}, u \in \mathcal{K}_s} \{ \bar{\Gamma}_{c,k}(\bar{\mathbf{f}}), \bar{R}_{c,u}(\bar{\mathbf{f}}) \} \\ & \simeq -\mu \log \left[\frac{1}{K^{\text{sat}}} \left\{ \sum_{j=1}^{K_t} \exp \left(\frac{\bar{\Gamma}_{c,j}(\bar{\mathbf{f}})}{-\mu} \right) + \sum_{i=1}^{K_s} \exp \left(\frac{\bar{R}_{c,i}(\bar{\mathbf{f}})}{-\mu} \right) \right\} \right], \end{aligned} \quad (56)$$

where μ is the accuracy of the LSE technique. As we set large μ , (56) becomes tight. This leads to the following problem:

$$\mathcal{P}_3 : \underset{\bar{\mathbf{f}}, \bar{\mathbf{v}}}{\text{maximize}} \left[-\mu \log \left[\frac{1}{K^{\text{sat}}} \left\{ \sum_{j=1}^{K_t} \exp \left(\frac{\bar{\Gamma}_{c,j}(\bar{\mathbf{f}})}{-\mu} \right) + \sum_{i=1}^{K_s} \exp \left(\frac{\bar{R}_{c,i}(\bar{\mathbf{f}})}{-\mu} \right) \right\} \right] \right] \\ + \sum_{i=1}^{K_s} \bar{\Gamma}_{p,i}(\bar{\mathbf{f}}) + \sum_{j=1}^{K_t} \bar{\Gamma}_{p,j}(\bar{\mathbf{v}}) \quad (57)$$

B. First-Order Optimality Condition

To get the solution for (57), we derive the first-order optimality conditions in the following lemma.

Lemma 1. Note that the Lagrangian function of (57) is (58), as shown at the top of the next page. To find a stationary point, we take the partial derivatives of $f(\bar{\mathbf{f}}, \bar{\mathbf{v}})$ with according to $\bar{\mathbf{f}}$ and $\bar{\mathbf{v}}$, then set it to zero, respectively, i.e., $\frac{\partial f(\bar{\mathbf{f}}, \bar{\mathbf{v}})}{\partial \bar{\mathbf{f}}} = 0$ and $\frac{\partial f(\bar{\mathbf{f}}, \bar{\mathbf{v}})}{\partial \bar{\mathbf{v}}} = 0$. For simplicity, we define the first and the second part of the Lagrangian function (58) as respectively $f_1(\bar{\mathbf{f}})$ and $f_2(\bar{\mathbf{v}})$.

First, we obtain the partial derivative of $f_1(\bar{\mathbf{f}})$ as given by (59) at the top of the next page, where

$$\begin{aligned} \mathbf{X}_{c,k}^{\text{bs}} &= \mathbf{S}_{c,k}^{\text{bs}} + \mathbf{C}_{c,k}^{\text{bs}} + \omega_k \mathbf{I}_{M(K_s+1)}, \quad \mathbf{Y}_{c,k}^{\text{bs}} = \mathbf{C}_{c,k}^{\text{bs}} + \omega_k \mathbf{I}_{M(K_s+1)}, \\ \mathbf{X}_{c,u}^{\text{sat}} &= \mathbf{S}_{c,u}^{\text{sat}} + \mathbf{U}_{c,u}^{\text{sat}} \end{aligned} \quad (60)$$

$$L(\bar{\mathbf{f}}) = \left\{ \prod_{j=1}^{K_t} \bar{\mathbf{f}}^H (\mathbf{C}_{p,j}^{\text{bs}} + \epsilon_j \mathbf{I}_{M(K_s+1)}) \bar{\mathbf{f}} \right\}^{\frac{1}{K_s}}. \quad (61)$$

To satisfy the first-order KKT condition, we set $\frac{\partial f_1(\bar{\mathbf{f}})}{\partial \bar{\mathbf{f}}} = 0$, and then rearrange it as

$$\mathbf{A}(\bar{\mathbf{f}}) \bar{\mathbf{f}} = \lambda^{\text{sat}}(\bar{\mathbf{f}}) \mathbf{B}(\bar{\mathbf{f}}) \bar{\mathbf{f}}, \quad (62)$$

where $\lambda^{\text{sat}}(\bar{\mathbf{f}})$, $\mathbf{A}(\bar{\mathbf{f}})$ and $\mathbf{B}(\bar{\mathbf{f}})$ are represented by

$$\begin{aligned} \lambda^{\text{sat}}(\bar{\mathbf{f}}) &= \left[\frac{1}{K^{\text{sat}}} \left\{ \sum_{j=1}^{K_t} \exp \left(\frac{\bar{\Gamma}_{c,j}(\bar{\mathbf{f}})}{-\mu} \right) + \sum_{i=1}^{K_s} \exp \left(\frac{\bar{R}_{c,i}(\bar{\mathbf{f}})}{-\mu} \right) \right\} \right]^{-\frac{\mu}{\log_2 e}} \\ & \times \prod_{i=1}^{K_s} \bar{\Gamma}_{p,i}(\bar{\mathbf{f}}) = \frac{\lambda_1^{\text{sat}}(\bar{\mathbf{f}})}{\lambda_2^{\text{sat}}(\bar{\mathbf{f}})}, \end{aligned} \quad (63)$$

$$\begin{aligned} \mathbf{A}(\bar{\mathbf{f}}) &= \lambda_1^{\text{sat}}(\bar{\mathbf{f}}) \cdot \left[\sum_{u=1}^{K_s} \left\{ \frac{\exp \left(-\frac{1}{\mu} \log_2 \left(\frac{\bar{\mathbf{f}}^H \mathbf{X}_{c,u}^{\text{sat}} \bar{\mathbf{f}}}{\bar{\mathbf{f}}^H \mathbf{U}_{c,u}^{\text{sat}} \bar{\mathbf{f}}} \right) \right)}{\sum_{i=1}^{K_s} \exp \left(-\frac{1}{\mu} \log_2 \left(\frac{\bar{\mathbf{f}}^H \mathbf{X}_{c,i}^{\text{sat}} \bar{\mathbf{f}}}{\bar{\mathbf{f}}^H \mathbf{U}_{c,i}^{\text{sat}} \bar{\mathbf{f}}} \right) \right)} \right\} \right. \\ & \left. + \frac{\mathbf{S}_{p,u}^{\text{sat}} + \mathbf{U}_{p,u}^{\text{sat}}}{\bar{\mathbf{f}}^H (\mathbf{S}_{p,u}^{\text{sat}} + \mathbf{U}_{p,u}^{\text{sat}}) \bar{\mathbf{f}} \cdot L(\bar{\mathbf{f}})} + \frac{L(\bar{\mathbf{f}})}{\nabla_{\bar{\mathbf{f}}} L(\bar{\mathbf{f}}) \bar{\mathbf{f}}} \right] \\ & + \sum_{k=1}^{K_t} \left\{ \frac{\exp \left(-\frac{1}{\mu} \log_2 \left(\frac{\bar{\mathbf{f}}^H \mathbf{X}_{c,k}^{\text{bs}} \bar{\mathbf{f}}}{\bar{\mathbf{f}}^H \mathbf{Y}_{c,k}^{\text{bs}} \bar{\mathbf{f}}} \right) \right)}{\sum_{j=1}^{K_t} \exp \left(-\frac{1}{\mu} \log_2 \left(\frac{\bar{\mathbf{f}}^H \mathbf{X}_{c,j}^{\text{bs}} \bar{\mathbf{f}}}{\bar{\mathbf{f}}^H \mathbf{Y}_{c,j}^{\text{bs}} \bar{\mathbf{f}}} \right) \right)} \right\}, \end{aligned} \quad (64)$$

$$f(\bar{\mathbf{f}}, \bar{\mathbf{v}}) = -\mu \log \underbrace{\left[\frac{1}{K_{\text{sat}}} \left\{ \sum_{j=1}^{K_t} \exp \left(\frac{\bar{\Gamma}_{c,j}(\bar{\mathbf{f}})}{-\mu} \right) + \sum_{i=1}^{K_s} \exp \left(\frac{\bar{R}_{c,i}(\bar{\mathbf{f}})}{-\mu} \right) \right\} \right]}_{f_1(\bar{\mathbf{f}})} + \underbrace{\sum_{i=1}^{K_s} \bar{\Gamma}_{p,i}(\bar{\mathbf{f}}) + \sum_{j=1}^{K_t} \bar{\Gamma}_{p,j}(\bar{\mathbf{v}})}_{f_2(\bar{\mathbf{v}})}. \quad (58)$$

$$\begin{aligned} \frac{\partial f_1(\bar{\mathbf{f}})}{\partial \bar{\mathbf{f}}} &= \frac{1}{\log 2} \sum_{u=1}^{K_s} \left(\frac{(\mathbf{S}_{p,u}^{\text{sat}} + \mathbf{U}_{p,u}^{\text{sat}})\bar{\mathbf{f}}}{\bar{\mathbf{f}}^H(\mathbf{S}_{p,u}^{\text{sat}} + \mathbf{U}_{p,u}^{\text{sat}})\bar{\mathbf{f}}} - \frac{\mathbf{U}_{p,u}^{\text{sat}}\bar{\mathbf{f}}}{\bar{\mathbf{f}}^H\mathbf{U}_{p,u}^{\text{sat}}\bar{\mathbf{f}}} + \frac{L(\bar{\mathbf{f}})}{\nabla_{\bar{\mathbf{f}}} L(\bar{\mathbf{f}})} \right) \\ &+ \sum_{k=1}^{K_t} \left\{ \frac{\exp \left(-\frac{1}{\mu} \log_2 \left(\frac{\bar{\mathbf{f}}^H \mathbf{X}_{c,k}^{\text{sat}} \bar{\mathbf{f}}}{\bar{\mathbf{f}}^H \mathbf{Y}_{c,k}^{\text{bs}} \bar{\mathbf{f}}} \right) \right) \left(\frac{\mathbf{X}_{c,k}^{\text{bs}} \bar{\mathbf{f}}}{\bar{\mathbf{f}}^H \mathbf{X}_{c,k}^{\text{bs}} \bar{\mathbf{f}}} - \frac{\mathbf{Y}_{c,k}^{\text{bs}} \bar{\mathbf{f}}}{\bar{\mathbf{f}}^H \mathbf{Y}_{c,k}^{\text{bs}} \bar{\mathbf{f}}} \right)}{\log 2 \cdot \sum_{j=1}^{K_t} \exp \left(-\frac{1}{\mu} \log_2 \left(\frac{\bar{\mathbf{f}}^H \mathbf{X}_{c,j}^{\text{sat}} \bar{\mathbf{f}}}{\bar{\mathbf{f}}^H \mathbf{Y}_{c,j}^{\text{bs}} \bar{\mathbf{f}}} \right) \right)} \right\} + \sum_{u=1}^{K_s} \left\{ \frac{\exp \left(-\frac{1}{\mu} \log_2 \left(\frac{\bar{\mathbf{f}}^H \mathbf{X}_{c,u}^{\text{sat}} \bar{\mathbf{f}}}{\bar{\mathbf{f}}^H \mathbf{U}_{c,u}^{\text{sat}} \bar{\mathbf{f}}} \right) \right) \left(\frac{\mathbf{X}_{c,u}^{\text{sat}} \bar{\mathbf{f}}}{\bar{\mathbf{f}}^H \mathbf{X}_{c,u}^{\text{sat}} \bar{\mathbf{f}}} - \frac{\mathbf{U}_{c,u}^{\text{sat}} \bar{\mathbf{f}}}{\bar{\mathbf{f}}^H \mathbf{U}_{c,u}^{\text{sat}} \bar{\mathbf{f}}} \right)}{\log 2 \cdot \sum_{i=1}^{K_s} \exp \left(-\frac{1}{\mu} \log_2 \left(\frac{\bar{\mathbf{f}}^H \mathbf{X}_{c,i}^{\text{sat}} \bar{\mathbf{f}}}{\bar{\mathbf{f}}^H \mathbf{U}_{c,i}^{\text{sat}} \bar{\mathbf{f}}} \right) \right)} \right\}, \end{aligned} \quad (59)$$

$$\begin{aligned} \mathbf{B}(\bar{\mathbf{f}}) &= \lambda_2^{\text{sat}}(\bar{\mathbf{f}}) \cdot \left[\sum_{u=1}^{K_s} \left\{ \frac{\exp \left(-\frac{1}{\mu} \log_2 \left(\frac{\bar{\mathbf{f}}^H \mathbf{X}_{c,u}^{\text{sat}} \bar{\mathbf{f}}}{\bar{\mathbf{f}}^H \mathbf{U}_{c,u}^{\text{sat}} \bar{\mathbf{f}}} \right) \right) \frac{\mathbf{U}_{c,u}^{\text{sat}}}{\bar{\mathbf{f}}^H \mathbf{U}_{c,u}^{\text{sat}} \bar{\mathbf{f}}}}{\sum_{i=1}^{K_s} \exp \left(-\frac{1}{\mu} \log_2 \left(\frac{\bar{\mathbf{f}}^H \mathbf{X}_{c,i}^{\text{sat}} \bar{\mathbf{f}}}{\bar{\mathbf{f}}^H \mathbf{U}_{c,i}^{\text{sat}} \bar{\mathbf{f}}} \right) \right)} \right. \right. \\ &+ \left. \left. \frac{\mathbf{U}_{p,u}^{\text{sat}}}{\bar{\mathbf{f}}^H \mathbf{U}_{p,u}^{\text{sat}} \bar{\mathbf{f}} \cdot L(\bar{\mathbf{f}})} \right\} + \sum_{k=1}^{K_t} \left\{ \frac{\exp \left(-\frac{1}{\mu} \log_2 \left(\frac{\bar{\mathbf{f}}^H \mathbf{X}_{c,k}^{\text{bs}} \bar{\mathbf{f}}}{\bar{\mathbf{f}}^H \mathbf{Y}_{c,k}^{\text{bs}} \bar{\mathbf{f}}} \right) \right) \frac{\mathbf{Y}_{c,k}^{\text{bs}}}{\bar{\mathbf{f}}^H \mathbf{Y}_{c,k}^{\text{bs}} \bar{\mathbf{f}}}}{\sum_{j=1}^{K_t} \exp \left(-\frac{1}{\mu} \log_2 \left(\frac{\bar{\mathbf{f}}^H \mathbf{X}_{c,j}^{\text{bs}} \bar{\mathbf{f}}}{\bar{\mathbf{f}}^H \mathbf{Y}_{c,j}^{\text{bs}} \bar{\mathbf{f}}} \right) \right)} \right\} \right]. \end{aligned} \quad (65)$$

As a result, the first-order KKT condition of $f_1(\bar{\mathbf{f}})$ regarding $\bar{\mathbf{f}}$ is satisfied if the following holds:

$$\mathbf{A}(\bar{\mathbf{f}})\bar{\mathbf{f}} = \lambda^{\text{sat}}(\bar{\mathbf{f}})\mathbf{B}(\bar{\mathbf{f}})\bar{\mathbf{f}} \Leftrightarrow \mathbf{B}^{-1}(\bar{\mathbf{f}})\mathbf{A}(\bar{\mathbf{f}})\bar{\mathbf{f}} = \lambda^{\text{sat}}(\bar{\mathbf{f}})\bar{\mathbf{f}}. \quad (66)$$

Second, for $\bar{\mathbf{v}}$, we follow a similar approach as above. We calculate the partial derivative of $f_2(\bar{\mathbf{v}})$, and then, use the first-order KKT condition, i.e., $\frac{\partial f_2(\bar{\mathbf{v}})}{\partial \bar{\mathbf{v}}} = 0$. As a result, the first-order KKT condition of $f_2(\bar{\mathbf{v}})$ regarding $\bar{\mathbf{v}}$ is satisfied if the following holds:

$$\mathbf{D}^{-1}(\bar{\mathbf{v}})\mathbf{C}(\bar{\mathbf{v}})\bar{\mathbf{v}} = \lambda^{\text{bs}}(\bar{\mathbf{v}})\bar{\mathbf{v}}, \quad (67)$$

where $\lambda^{\text{bs}}(\bar{\mathbf{v}})$, $\mathbf{C}(\bar{\mathbf{v}})$ and $\mathbf{D}(\bar{\mathbf{v}})$ are given by

$$\lambda^{\text{bs}}(\bar{\mathbf{v}}) = \prod_{j=1}^{K_t} \bar{\Gamma}_{p,j}(\bar{\mathbf{v}}) = \frac{\lambda_1^{\text{bs}}(\bar{\mathbf{v}})}{\lambda_2^{\text{bs}}(\bar{\mathbf{v}})}, \quad (68)$$

$$\mathbf{C}(\bar{\mathbf{v}}) = \lambda_1^{\text{bs}}(\bar{\mathbf{v}}) \sum_{j=1}^{K_t} \left(\frac{\mathbf{S}_{p,j}^{\text{bs}}}{\bar{\mathbf{v}}^H \mathbf{S}_{p,j}^{\text{bs}} \bar{\mathbf{v}}} \right), \mathbf{D}(\bar{\mathbf{v}}) = \lambda_2^{\text{bs}}(\bar{\mathbf{v}}) \sum_{j=1}^{K_t} \left(\frac{\mathbf{U}_{p,j}^{\text{bs}}}{\bar{\mathbf{v}}^H \mathbf{U}_{p,j}^{\text{bs}} \bar{\mathbf{v}}} \right). \quad (69)$$

In Lemma 1, the first important observation is that the optimality conditions are decoupled into two parts, each of which is solely related to $\bar{\mathbf{f}}$ and $\bar{\mathbf{v}}$, respectively. To be specific, differentiating the Lagrangian function $f(\bar{\mathbf{f}}, \bar{\mathbf{v}})$ in (58) with regard to $\bar{\mathbf{f}}$, we have $\frac{\partial f(\bar{\mathbf{f}}, \bar{\mathbf{v}})}{\partial \bar{\mathbf{f}}} = g_1(\bar{\mathbf{f}})$, where $g_1(\bar{\mathbf{f}})$ is independent to $\bar{\mathbf{v}}$. Similar to this, we have $\frac{\partial f(\bar{\mathbf{f}}, \bar{\mathbf{v}})}{\partial \bar{\mathbf{v}}} = g_2(\bar{\mathbf{v}})$, where $g_2(\bar{\mathbf{v}})$ is independent to $\bar{\mathbf{f}}$. We note that this is done by our decoupling process described in Section III. Thanks to this decoupling, functions related to $\bar{\mathbf{f}}$ and $\bar{\mathbf{v}}$ can be independently computed in a distributed way.

Next we explain how to achieve the local optimal point for each of $\bar{\mathbf{f}}$ and $\bar{\mathbf{v}}$. Note that the first-order KKT condition

(66) (regarding $\bar{\mathbf{f}}$) and (67) (regarding $\bar{\mathbf{v}}$) are cast as a form of generalized nonlinear eigenvalue problems. Specifically, in (66), $\bar{\mathbf{f}}$ behaves as an eigenvector of the eigenvector-dependent matrix $\mathbf{B}^{-1}(\bar{\mathbf{f}})\mathbf{A}(\bar{\mathbf{f}})$, and in (67), $\bar{\mathbf{v}}$ acts as an eigenvector of the eigenvector-dependent matrix $\mathbf{D}^{-1}(\bar{\mathbf{v}})\mathbf{C}(\bar{\mathbf{v}})$. In this relation, the eigenvalue $\lambda^{\text{sat}}(\bar{\mathbf{f}})$ given by (63) corresponds to the $\bar{\mathbf{f}}$ -related term of the Lagrangian function $f_1(\bar{\mathbf{f}})$, while the eigenvalue $\lambda^{\text{bs}}(\bar{\mathbf{v}})$ given by (68) corresponds to the $\bar{\mathbf{v}}$ -related term of the Lagrangian function $f_2(\bar{\mathbf{v}})$. As a result, if we find the principal eigenvectors of (66) and (67), then we reach the maximum stationary point. By doing this, we maximize the objective function (57). Note that this generalized nonlinear eigenvalue problem is different from the classical eigenvalue problem in that the matrix is dependent on its eigenvector itself. In what follows, we propose an algorithm to find the principal eigenvectors of (66) and (67).

C. STIN-GPI

We propose a STIN-GPI algorithm based on the method developed in [30]. The process of the proposed algorithm is iteratively updating $\bar{\mathbf{f}}$ and $\bar{\mathbf{v}}$ by using the power iteration, while the matrix is computed with the previously obtained $\bar{\mathbf{f}}$ and $\bar{\mathbf{v}}$. In our method, STIN-GPI consists of two stages, where the first stage is performed in the LEO satellite for designing $\bar{\mathbf{f}}$ and the second stage is performed in the terrestrial BS for designing $\bar{\mathbf{v}}$. We mention that these two stages are totally departed; so that no outcome of one stage goes into the other stage as the input. In the first stage with a given $\bar{\mathbf{f}}^{(t-1)}$ obtained in the $(t-1)$ -th iteration, we calculate the matrices $\mathbf{A}(\bar{\mathbf{f}}^{(t-1)})$ and $\mathbf{B}(\bar{\mathbf{f}}^{(t-1)})$ utilizing (64) and (65). Then, we update $\bar{\mathbf{f}}^{(t)}$ in the t -th iteration by $\bar{\mathbf{f}}^{(t)} = \frac{\mathbf{B}^{-1}(\bar{\mathbf{f}}^{(t-1)})\mathbf{A}(\bar{\mathbf{f}}^{(t-1)})\bar{\mathbf{f}}^{(t-1)}}{\|\mathbf{B}^{-1}(\bar{\mathbf{f}}^{(t-1)})\mathbf{A}(\bar{\mathbf{f}}^{(t-1)})\bar{\mathbf{f}}^{(t-1)}\|}$. This process repeats until convergence under a predetermined tolerance value ζ , i.e., $\|\bar{\mathbf{f}}^{(t)} - \bar{\mathbf{f}}^{(t-1)}\| < \zeta$. The second stage runs with the same way. The matrices $\mathbf{C}(\bar{\mathbf{v}}^{(t-1)})$ and $\mathbf{D}(\bar{\mathbf{v}}^{(t-1)})$ are calculated using $\bar{\mathbf{v}}^{(t-1)}$. Then it is updated by $\bar{\mathbf{v}}^{(t)} = \frac{\mathbf{D}^{-1}(\bar{\mathbf{v}}^{(t-1)})\mathbf{C}(\bar{\mathbf{v}}^{(t-1)})\bar{\mathbf{v}}^{(t-1)}}{\|\mathbf{D}^{-1}(\bar{\mathbf{v}}^{(t-1)})\mathbf{C}(\bar{\mathbf{v}}^{(t-1)})\bar{\mathbf{v}}^{(t-1)}\|}$. This process repeats until $\|\bar{\mathbf{v}}^{(t)} - \bar{\mathbf{v}}^{(t-1)}\| < \zeta$. We describe the whole process of our proposed method in Algorithm 1.

We note that the convergence speed of the proposed STIN-GPI is tied to μ . Specifically, if μ takes on a very large value, the smoothness of the LSE approximation is degraded,

Algorithm 1: STIN-GPI algorithm

```

Initialize:  $\bar{\mathbf{f}}^{(0)} = (\text{MRT})$ ,  $\bar{\mathbf{v}}^{(0)} = (\text{MRT})$ ,  $t = 1$ 
repeat
  Stage 1. LEO Satellite Beamforming Design
  repeat
    Calculate  $\mathbf{A}(\bar{\mathbf{f}}^{(t-1)})$ ,  $\mathbf{B}(\bar{\mathbf{f}}^{(t-1)})$ 
    Obtain  $\bar{\mathbf{f}}^{(t)} \leftarrow \frac{\mathbf{B}^{-1}(\bar{\mathbf{f}}^{(t-1)})\mathbf{A}(\bar{\mathbf{f}}^{(t-1)})\bar{\mathbf{f}}^{(t-1)}}{\|\mathbf{B}^{-1}(\bar{\mathbf{f}}^{(t-1)})\mathbf{A}(\bar{\mathbf{f}}^{(t-1)})\bar{\mathbf{f}}^{(t-1)}\|}$ 
  until  $\|\bar{\mathbf{f}}^{(t)} - \bar{\mathbf{f}}^{(t-1)}\| < \zeta$ ;
  Stage 2. Terrestrial BS Beamforming Design
  repeat
    Calculate  $\mathbf{C}(\bar{\mathbf{v}}^{(t-1)})$ ,  $\mathbf{D}(\bar{\mathbf{v}}^{(t-1)})$ 
    Obtain  $\bar{\mathbf{v}}^{(t)} \leftarrow \frac{\mathbf{D}^{-1}(\bar{\mathbf{v}}^{(t-1)})\mathbf{C}(\bar{\mathbf{v}}^{(t-1)})\bar{\mathbf{v}}^{(t-1)}}{\|\mathbf{D}^{-1}(\bar{\mathbf{v}}^{(t-1)})\mathbf{C}(\bar{\mathbf{v}}^{(t-1)})\bar{\mathbf{v}}^{(t-1)}\|}$ 
  until  $\|\bar{\mathbf{v}}^{(t)} - \bar{\mathbf{v}}^{(t-1)}\| < \zeta$ ;
   $t \leftarrow t + 1$ 
until  $t = t^{\max}$ ;
Output:  $\bar{\mathbf{f}}^{(t^{\max})}, \bar{\mathbf{v}}^{(t^{\max})}$ 

```

resulting in slow convergence. To address this, we adjust μ for facilitating the convergence. For instance, we can incrementally decrease μ if the algorithm does not converge within predetermined iterations.

Remark 2. (Algorithm complexity) In a big-O sense, the total computational complexity of the proposed STIN-GPI algorithm is dominated by the calculation of $\mathbf{B}^{-1}(\bar{\mathbf{f}})$ and $\mathbf{D}^{-1}(\bar{\mathbf{v}})$. The matrix $\mathbf{B}(\bar{\mathbf{f}})$ is expressed as the sum of the block diagonal matrices of $\{\mathbf{S}_{c,k}^{\text{bs}}, \mathbf{C}_{c,k}^{\text{bs}}, \mathbf{S}_{c,u}^{\text{sat}}, \mathbf{U}_{c,u}^{\text{sat}}\} \in \mathbb{C}^{M(K_s+1) \times M(K_s+1)}$. Since the inverse matrix of $\mathbf{B}^{-1}(\bar{\mathbf{f}})$ can be calculated using the inverse of each submatrix, the total computational complexity is with the order of $\mathcal{O}(\frac{1}{3}(K_s+1)M^3)$. Similar to this way, in case of stage 2, the computational complexity of the inverse matrix $\mathbf{D}^{-1}(\bar{\mathbf{v}})$ is $\mathcal{O}(\frac{1}{3}K_tN^3)$. For this reason, the complexity of the proposed STIN-GPI per iteration scales with the order of $\mathcal{O}(\frac{1}{3}(K_sM^3 + K_tN^3))$ when K_s, M, K_t and N increase with the same order.

Remark 3. (Generalization to multi-layer RS strategy) Even though we only consider the 1-layer RS strategy, it is possible to generalize this to the multi-layer RS strategy. For instance, we construct three-types of common streams, such as s_c , s_c^{sat} and s_c^{bs} . Upon this, we make s_c^{sat} to be decoded by the SUs in \mathcal{K}_s and s_c^{bs} to be decoded by the TUs in \mathcal{K}_t (and same s_c). By doing this, we efficiently mitigate the IUI among users as well as ICI, which leads to improve performance. To design the precoder in such multi-layer RS strategy cases, we can extend it to our scenario by additionally constructing $\mathbf{f}_c^{\text{sat}} \in \mathbb{C}^M$ and $\mathbf{f}_c^{\text{bs}} \in \mathbb{C}^M$, and then reassembling it into higher-dimensional vector as described in (30). For conciseness of the paper and page limitation, we only focus on the 1-layer RS strategy.

V. NUMERICAL RESULTS

In this section, we evaluate the spectral efficiency performance of the proposed method via numerical simulations. To this end, we consider the following STIN simulation scenario. The STIN uses the Ka-band as operating bandwidth [21], [25], [35]. The radius of the LEO satellite coverage region

is 500km, while the radius of terrestrial BS coverage is 50km and the height of terrestrial BS is 30m. SUs and TUs are uniformly distributed within their respective coverage areas. The simulation setups are: $f_c = 20\text{GHz}$, $B_w = 800\text{MHz}$, $d_0^{\text{sat}} = 1000\text{km}$, $G_{\text{sat}} = 6\text{dBi}$, $G_u = 0\text{dBi}$, $d_1^{\text{sat}} = d_2^{\text{sat}} = \lambda$, $d_1^{\text{bs}} = d_2^{\text{bs}} = \frac{\lambda}{2}$, $L_t = 10$, $M_1 = 5$, $M_2 = 5$, $N_1 = 3$, $N_2 = 3$, $K_s = 10$, $K_t = 3$, $K_t^{\text{int}} = 1$, $\mu = 0.1$, $\tau p^{\text{pi}} = 2$, $\rho = 4$, $\zeta = 0.01$ and $t^{\max} = 1000$, unless mentioned otherwise. As baseline methods, we consider the followings:

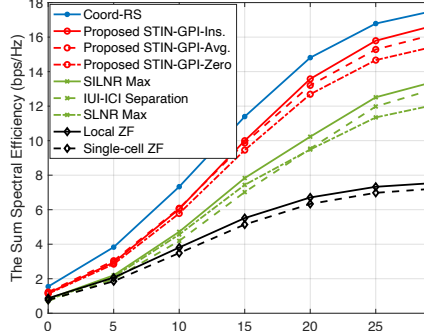
- **Coordinated Precoding with RS (Coord-RS)** [5]: In this method, we find the optimal precoder to solve \mathcal{P}_1 in a coordinated fashion, i.e., by sharing CSIT, while incorporating the RS strategy. The basic setup of Coord-RS corresponds to [5], except that [5] maximizes the minimum spectral efficiency while Coord-RS maximizes the sum spectral efficiency.
- **SILNR Max** [13]: This method adopts the SILNR instead of the exact SINR for distributed design.
- **IUI-ICI Separation** [12]: This method decouples the IUI and the ICI based on the high SNR assumption. Subsequently, the sum spectral efficiency maximization is performed without using the RS strategy.
- **SLNR Max** [6]: The SLNR is adopted as an alternative of the exact SINR.
- **Local ZF** [36]: This method not only mitigates the IUI using the classical zero-forcing (ZF) but also mitigates the ICI; this is done by projecting a precoding vector to null space of IUI and ICI by using the remaining spatial degrees-of-freedom.
- **Single-cell ZF**: This method is classical ZF that only suppresses the IUI.

We clarify that, including the proposed STIN-GPI, SILNR Max, IUI-ICI Separation, SLNR Max, Local ZF, Single-cell ZF are distributed method that does not require CSIT sharing, while Coord-RS is a coordinated method. For the proposed STIN-GPI method, we consider 3 different versions depending on the report mechanisms:

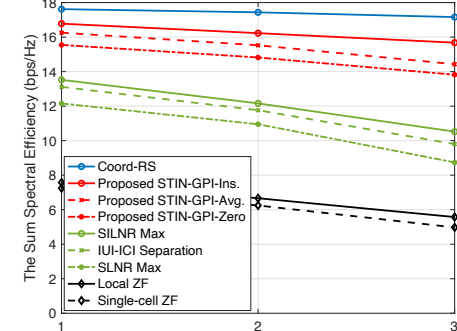
- **STIN-GPI-Ins.** : As mentioned in Remark 1, the TUs in $\mathcal{K}_t^{\text{int}}$ report the instantaneous received signal power $\bar{\mathbf{v}}^H \mathbf{U}_{c,k}^{\text{bs}} \bar{\mathbf{v}}$ to the LEO satellite; so that the STIN-GPI exploits the exact instantaneous interference information.
- **STIN-GPI-Avg.** : In (46) and (53), we repeatedly form the channel vector for TU k and use it to generate 1000 data samples $\mathbf{U}_{p,k}^{\text{bs}}$ and $\mathbf{U}_{c,k}^{\text{bs}}$. Then, we design $\bar{\mathbf{v}}$, multiply it with $\mathbf{U}_{p,k}^{\text{bs}}$ and $\mathbf{U}_{c,k}^{\text{bs}}$, and finally average to obtain $\mathbb{E}[\bar{\mathbf{v}}^H \mathbf{U}_{p,k}^{\text{bs}} \bar{\mathbf{v}}] = \epsilon_k$ and $\mathbb{E}[\bar{\mathbf{v}}^H \mathbf{U}_{c,k}^{\text{bs}} \bar{\mathbf{v}}] = \omega_k$. As a result, the STIN-GPI uses the averaged interference information.
- **STIN-GPI-Zero** : This method forcibly decouples the functions for $\bar{\mathbf{f}}$ and $\bar{\mathbf{v}}$ by assuming zero IUI ($\epsilon_k = 0$) and zero ICI ($\omega_k = 0$). In this case, the STIN-GPI does not use the interference information.

The simulation results are demonstrated as follows:

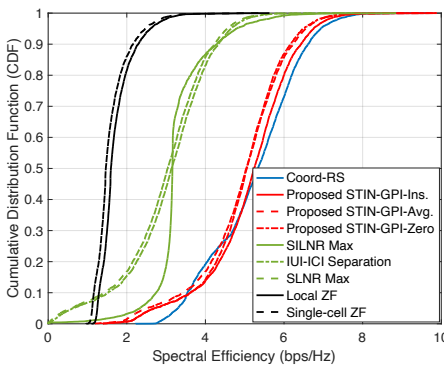
Link-level simulation: Fig. 2(a) shows how the ergodic sum spectral efficiency per SNR. We first observe that, in the proposed methods, the spectral efficiency performance order is STIN-GPI-Ins. > STIN-GPI-Avg. > STIN-GPI-Zero. This is reasonable because STIN-GPI-Ins. exploits exact instan-



(a)



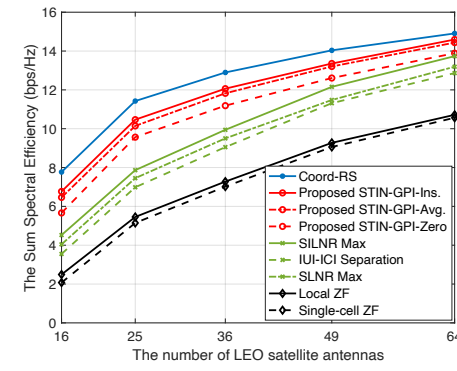
(a)



(b)

Fig. 2. Link-level and system-level simulations between the proposed distributed STIN-GPI and baseline methods. (a) Comparison of sum spectral efficiency per SNR. (b) Comparison of CDF per user's spectral efficiency.

taneous interference information, while STIN-GPI-Avg. only uses the averaged one and STIN-GPI-Zero does not use any information in designing precoders. However, STIN-GPI-Ins. requires instantaneous interference reporting from the TUs, incurring a substantial amount of overhead. Unlike this, STIN-GPI-Avg. merely needs to deliver the constant ϵ_k and ω_k that does not vary over channels, thus the associated overheads are significantly smaller than those of STIN-GPI-Ins. Considering the trade-off between the performance gains and the associated overheads, STIN-GPI-Avg. is the most favorable option. Therefore, Fig. 2(a) shows that the STIN-GPI-Avg. offers around 20% and 29% gains at SNR = 30dB over the SILNR Max and the SLNR Max, respectively. These gains stem from two perspectives: i) Our method enables to perform SIC at the TUs by using the RS strategy. If the interference from the LEO satellite persists due to imperfect CSIT estimation, the TUs encounter severe performance deterioration. Through the RS strategy, TUs can eliminate this interference by means of SIC, by which significant spectral efficiency gains are attainable. ii) In the decoupling process of our method, we take average to the IUI term to disentangle the ICI term from the sum spectral efficiency. This is meticulous treatment that establishes a lower bound on the spectral efficiency, aptly encompassing the interference's influence. In the case of SLNR approach, only the leakage term is considered, which cannot count the effect of the interference in a proper way. This brings the spectral



(b)

Fig. 3. Comparison of sum spectral efficiency among different strategies under the assumption of SNR = 15dB (a) per the number of TUs experiencing interference from the satellite (K_t^{int}), (b) per the number of LEO satellite antennas to $M = 16, 25, 36, 49, 64$.

efficiency improvement to our method.

System-level simulation: We conduct system-level simulations. Fig. 2(b) shows the cumulative distribution function (CDF) for the spectral efficiency. Compared to the SILNR Max, IUI-ICI Separation and SLNR Max methods, the 95-percentile user's spectral efficiency with STIN-GPI-Avg. increases by about 37%, 40% and 44%, respectively. Furthermore, we observe a performance difference of approximately 5% in the 95-percentile user's spectral efficiency between Coord-RS and STIN-GPI-Avg.. However, in the case of STIN-GPI-Ins., the performance difference in the 95-percentile user's spectral efficiency compared to the Coord-RS method reduces to 3%. This means that our method, assisted by the instantaneous reporting, achieves comparable performances to those of the coordinated approach even in the absence of CSIT sharing.

Per K_t^{int} and M : Fig. 3(a) demonstrates the comparison of sum spectral efficiency per the number of TUs K_t^{int} that experiences the interference from the LEO satellite. By increasing the radius of the LEO satellite coverage area to 500km, 520km, and 550km, K_t^{int} is set to increase from 1 to 3. We observe that our proposed STIN-GPI-Ins. method worsens by 7%, while other methods (SILNR Max, IUI-ICI Separation, SLNR Max) that do not use the RS strategy worsen by 28%, 33%, and 39%, respectively. The rationale behind these gains lies in the RS strategy's capability to effectively mitigate ICI, making it

robust against the increased ICI.

To shed light on the performance in the large-scale antenna regime, we show the sum spectral efficiency per the number of the LEO satellite antennas in Fig. 3(b). The figure shows that proposed STIN-GPI-Avg. method outperforms the SILNR Max, IUI-ICI Separation and SLNR Max methods by around 16%, 22% and 29%, respectively. Furthermore, the proposed STIN-GPI-Ins. method, which applies the reporting regime, achieves a performance gain of 8%. However, this gap gets smaller as the number of transmit antennas increases. This is due to the increasing spatial degrees-of-freedom resulting from a larger number of antennas, leading to enhanced overall throughput gains. Nevertheless, we observe that our proposed STIN-GPI methods outperform other methods that do not use RS strategy in all antenna regions; meaning that our method is suitable in massive MIMO systems.

VI. CONCLUSIONS

In this paper, we propose a novel distributed precoding approach using RS strategy. Our key idea is to decouple the sum spectral efficiency into two separated terms, each of which is a only function of the satellite's precoder and the terrestrial BS's precoder, respectively. Based on the distributed optimization problem, we approximate the non-smooth objective function by using the LSE technique, thereafter develop the STIN-GPI algorithm that finds the best local optimal point. The simulation results show that the proposed STIN-GPI method achieves around 20 ~ 29% spectral efficiency gains over the existing distributed precoding methods. In future work, we plan to extend this work by incorporating a multi-satellites and multi-BSs environment.

REFERENCES

- [1] A. Lozano *et al.*, “Fundamental limits of cooperation,” *IEEE Trans. Inf. Theory*, vol. 59, no. 9, pp. 5213–5226, 2013.
- [2] D. Gesbert *et al.*, “Multi-cell MIMO cooperative networks: A new look at interference,” *IEEE J. Sel. Areas Commun.*, vol. 28, no. 9, pp. 1380–1408, 2010.
- [3] J. Park *et al.*, “Unified modeling and rate coverage analysis for satellite-terrestrial integrated networks: Coverage extension or data offloading?” 2023. [Online]. Available: <https://arxiv.org/abs/2307.03343>
- [4] M. A. Vazquez *et al.*, “Precoding in multibeam satellite communications: Present and future challenges,” *IEEE Wireless Communications*, vol. 23, no. 6, pp. 88–95, 2016.
- [5] L. Yin and B. Clerckx, “Rate-splitting multiple access for satellite-terrestrial integrated networks: Benefits of coordination and cooperation,” *IEEE Trans. Wireless Commun.*, vol. 22, no. 1, pp. 317–332, 2023.
- [6] M. Sadek, A. Tarighat, and A. H. Sayed, “A leakage-based precoding scheme for downlink multi-user MIMO channels,” *IEEE Trans. Wireless Commun.*, vol. 6, no. 5, pp. 1711–1721, 2007.
- [7] R. Zakhour and D. Gesbert, “Coordination on the MISO interference channel using the virtual SINR framework,” in *2009 International ITG Workshop on Smart Antennas (WSA)*, 2009.
- [8] R. Zakhour and D. Gesbert, “Distributed multicell-MISO precoding using the layered virtual SINR framework,” *IEEE Transactions on Wireless Communications*, vol. 9, no. 8, pp. 2444–2448, 2010.
- [9] Björnson *et al.*, “Cooperative multicell precoding: Rate region characterization and distributed strategies with instantaneous and statistical CSI,” *IEEE Trans. Signal Process.*, vol. 58, no. 8, pp. 4298–4310, 2010.
- [10] S. He, Y. Huang, H. Wang, S. Jin, and L. Yang, “Leakage-aware energy-efficient beamforming for heterogeneous multicell multiuser systems,” *IEEE J. Sel. Areas Commun.*, vol. 32, no. 6, pp. 1268–1281, 2014.
- [11] T. X. Tran and K. C. Teh, “Spectral and energy efficiency analysis for SLNR precoding in massive MIMO systems with imperfect CSI,” *IEEE Trans. Wireless Commun.*, vol. 17, no. 6, pp. 4017–4027, 2018.
- [12] H.-J. Choi *et al.*, “Distributed beamforming techniques for weighted sum-rate maximization in MISO interfering broadcast channels,” *IEEE Transactions on Wireless Communications*, vol. 11, no. 4, pp. 1314–1320, 2012.
- [13] D. Han and N. Lee, “Distributed precoding using local CSIT for MU-MIMO heterogeneous cellular networks,” *IEEE Trans. Commun.*, vol. 69, no. 3, pp. 1666–1678, 2021.
- [14] J. Wang, M. Dong, B. Liang, G. Boudreau, and H. Abou-zeid, “Distributed coordinated precoding for MIMO cellular network virtualization,” *IEEE Trans. Wireless Commun.*, vol. 21, no. 1, pp. 106–120, 2022.
- [15] R. H. Etkin *et al.*, “Gaussian interference channel capacity to within one bit,” *IEEE Trans. Inf. Theory*, vol. 54, no. 12, pp. 5534–5562, 2008.
- [16] A. Bazco-Nogueras *et al.*, “Distributed CSIT does not reduce the generalized DoF of the 2-user MISO broadcast channel,” *IEEE Wireless Commun. Lett.*, vol. 8, no. 3, pp. 685–688, 2019.
- [17] J. Park *et al.*, “Rate-splitting multiple access for 6G networks: Ten promising scenarios and applications,” *accepted to IEEE Network*, 2023. [Online]. Available: <https://arxiv.org/abs/2306.12978>
- [18] Y. Xu *et al.*, “Distributed rate-splitting multiple access for multilayer satellite communications,” *arXiv preprint arXiv:2307.07382*, 2023.
- [19] H.-F. Chong *et al.*, “Capacity theorems for the “Z” channel,” *IEEE Trans. Inf. Theory*, vol. 53, no. 4, pp. 1348–1365, 2007.
- [20] L. You, K.-X. Li, J. Wang, X. Gao, X.-G. Xia, and B. Ottersten, “Massive MIMO transmission for LEO satellite communications,” *IEEE J. Sel. Areas Commun.*, vol. 38, no. 8, pp. 1851–1865, 2020.
- [21] K. Li *et al.*, “Downlink transmit design for massive MIMO LEO satellite communications,” *IEEE Trans. Commun.*, vol. 70, no. 2, pp. 1014–1028, 2022.
- [22] K. Li *et al.*, “Channel estimation for LEO satellite massive MIMO OFDM communications,” *IEEE Trans. Wireless Commun.*, pp. 1–1, 2023.
- [23] L. You *et al.*, “Hybrid analog/digital precoding for downlink massive MIMO LEO satellite communications,” *IEEE Trans. Wireless Commun.*, vol. 21, no. 8, pp. 5962–5976, 2022.
- [24] B. Vojcic, R. Pickholtz, and L. Milstein, “Performance of DS-CDMA with imperfect power control operating over a low earth orbiting satellite link,” *IEEE J. Sel. Areas Commun.*, vol. 12, no. 4, pp. 560–567, 1994.
- [25] 3GPP TR 38.811, “3rd generation partnership project; technical specification group radio access network; study on new radio (NR) to support non terrestrial networks (release 15),” *Tech. Rep. 3GPP TR 38.811 V15.0.0*, Jun. 2018.
- [26] A. Papathanasiou *et al.*, “A comparison study of the uplink performance of W-CDMA and OFDM for mobile multimedia communications via LEO satellites,” *IEEE Personal Commun.*, vol. 8, no. 3, pp. 35–43, 2001.
- [27] B. Zheng *et al.*, “Intelligent reflecting surface-aided LEO satellite communication: Cooperative passive beamforming and distributed channel estimation,” *IEEE Journal on Selected Areas in Communications*, vol. 40, no. 10, pp. 3057–3070, 2022.
- [28] O. Dizzdar, Y. Mao, and B. Clerckx, “Rate-splitting multiple access to mitigate the curse of mobility in (massive) MIMO networks,” *IEEE Trans. Commun.*, vol. 69, no. 10, pp. 6765–6780, 2021.
- [29] T. Kim, D. J. Love, and B. Clerckx, “MIMO systems with limited rate differential feedback in slowly varying channels,” *IEEE Trans. Commun.*, vol. 59, no. 4, pp. 1175–1189, 2011.
- [30] J. Park, J. Choi, N. Lee, W. Shin, and H. V. Poor, “Rate-splitting multiple access for downlink MIMO: A generalized power iteration approach,” *IEEE Trans. Wireless Commun.*, vol. 22, no. 3, pp. 1588–1603, 2023.
- [31] M. Ding and S. D. Blostein, “Maximum mutual information design for MIMO systems with imperfect channel knowledge,” *IEEE Trans. Inf. Theory*, vol. 56, no. 10, pp. 4793–4801, 2010.
- [32] D. Kim, J. Choi, J. Park, and D. K. Kim, “Max–Min fairness beamforming with rate-splitting multiple access: Optimization without a toolbox,” *IEEE Wireless Commun. Lett.*, vol. 12, no. 2, pp. 232–236, 2023.
- [33] H. Joudeh and B. Clerckx, “Sum-rate maximization for linearly precoded downlink multiuser MISO systems with partial CSIT: A rate-splitting approach,” *IEEE Trans. Commun.*, vol. 64, no. 11, pp. 4847–4861, 2016.
- [34] C. Shen and H. Li, “On the dual formulation of boosting algorithms,” *IEEE Trans. on Pattern Analysis and Machine Intelligence*, vol. 32, no. 12, pp. 2216–2231, 2010.
- [35] L. You *et al.*, “Beam squint-aware integrated sensing and communications for hybrid massive MIMO LEO satellite systems,” *IEEE J. Sel. Areas Commun.*, vol. 40, no. 10, pp. 2994–3009, 2022.
- [36] G. Interdonato, M. Karlsson, E. Björnson, and E. G. Larsson, “Local partial zero-forcing precoding for cell-free massive MIMO,” *IEEE Trans. Wireless Commun.*, vol. 19, no. 7, pp. 4758–4774, 2020.